The diorite, diorite porphyry and quartz diorite exposed in the upper stream of the Mamburao River subjected contact metamorphism to the limestone of the Sablayan group and Mansalay formation, and formed iron deposits.

The results of the microscopic examination are as follows.

Diorite (TR2–080)

Texture: Holocrystalline, equigranular.

Constituent minerals: Main minerals are plagioclase and hornblende. Plagioclase is 0.3 – 1.5 mm in size, and partially replaced by sericite. Hornblende shows pleochroism of brown to light brown. It is subhedral, being 0.3 – 2mm in size, and partly altered to chlorite, epidote and actinolite. Accessory opaque minerals and apatite, and secondary minerals of sphene and quartz are also observable.

Diorite porphyry (TR2–083)

Texture: Porphyritic texture.

Constituent minerals: Phenocrysts consist of plagioclase, potash-feldspar and augite. Plagioclase of 0.5 – 2.5 mm in size is euhedral to subhedral, and is replaced by albite, a little sericite and epidote. Potash-feldspar of 0.3 – 1.5 mm in size is subhedral to anhedral, and partly altered to albite. Augite is 0.3 – 1.5 mm in size, and most of all are changed to chlorite. Groundmass consists of albite with a little apatite and opaque minerals. Groundmass strongly undergoes albitization and epidotization, and abundant epidote and albite with a small amount of quartz and sericite occurred in it.

Quartz diorite (TR2–110)

Texture: Holocrystalline, equigranular.

Constituent minerals: Main minerals are composed of potash-feldspar, plagioclase, quartz and mafic minerals, and potash-feldspar is most abundant. Anhedral potash-feldspar is 0.3 – 1.5 mm in size, and partially altered to sericite. Euhedral to subhedral plagioclase is 0.4 – 3 mm in size, and remarkably undergoes sericitization. Quartz is anhedral and less than 0.6 mm in size, and show an undulatory extinction. Mafic minerals are subjected to alteration, and are replaced by chlorite, sericite and sphene.

Age: From the results of K–Ar dating on quartz diorite in Phase I, and the evidence that these rocks gave contact metamorphism to the limestone of Eocene age, it is concluded that these were intruded during Eocene to Oligocene time.

1–5 Chemical Composition of the Rocks

Fifty samples were selected for major elements bulk rock analysis in this phase. The results of analyses and their normative values are shown in Table I–4. For the normative calculation of the Ultramafic rocks, the method proposed by Hayashi (1968) was applied which has been modified from C.I.P.W. norm calculation sequence at the following three points.

1 FeO and Fe_2O_3 are added to equal amount of Cr_2O_3 and NiO respectively, to make chromite and trevorite.
2 Al_2O_3 which is remnant after calculation of feldspars, is added to equal amount of MgO in order to make spinel.
3 An excess of Fe_2O_3 after the calculation of acmite and trevorite is recalculated to FeO for olivine and pyroxene.

1–5–1 Chemical Characteristics of Halcon Metamorphics

As for Halcon metamorphics, two samples of green schist, two samples of mica schist and one sample of amphibolite were selected for chemical analyses. In the ACF diagram (Fig. I–9-1 ①), the results of chemical analyses show that green schist (KR2–112) and amphibolite (TR2–046) fall in the field of mafic igneous rock, and mica schist (TR2–161, FR2–073) and green schist (YR2–039), on the other hand, fall in that of pelitic rock and greywacke.

1–5–2 Chemical Characteristics of Basalt Lava of the Lumintao Formation and Associated Intrusive Rocks

Three samples of massive lava were chosen from the basalt lava of the Lumintao formation for chemical analyses. Besides them, three intrusive rocks, which are one sample of dolerite and two samples of gabbro, are also analyzed. The results of chemical analysis of these samples show that all of the samples of the Lumintao formation including intrusive rocks, having SiO_2 % range of 43.50 to 50.80, are compositionally basic and that all of them, except KR2–017 and KR2–092 which contain normative olivine, have normative quartz.

The results of chemical analyses were plotted in the ($Na_2O + K_2O$) – SiO_2 diagram (Fig. I–9-1 ②) and Total FeO – Total FeO/MgO diagram (Fig. I–9-1 ③, only for basalt). In these diagrams all the analyzed samples fall in the field of tholeiitic basalt and they seem to follow the trend line of differentiation of tholeiitic rocks in the AFM diagram (Fig. I–9-1 (4)). It is also suggested from the diagrams of solidification index (MgO x 100/(MgO + Fe_2O_3 + FeO + Na_2O + K_2O)) vs. Fe_2O_3 + FeO, TiO_2, Al_2O_3 and MgO (Fig. I–9-2 ⑤ – ⑧) that chemical variations of these rocks represent a differentiation trend of tholeiitic basalt magma. This is supported by such aspects that the dolerite has a similar chemical composition to that of the basalt, and that

Table I-4 Chemical Composition and C.I.P.W. Norm (1)

Rock Type		Ultramafic Complex (ultramafic rocks and associated rocks)															
		Pintin Body									Liwliw Body			Igsoso Body			
Location		Pintin R.	Pintin R.	Pintin R.	Pintin R.	Pintin R.	Pintin R.	Pintin R.	Pintin R.	Casiligan R.	Liwliw	Liwliw	Liwliw	Igsoso	Igsoso	Igsoso	Igsoso
Sample No.		KR2-020	KR2-021	KR2-026	KR2-033	KR2-040	KR2-48	KR2-030	KR2-036	SR2-140	KR2-54	KR2-077	KR2-078	KR2-061	KR2-063	KR2-064	KR2-066
Rock Name		harzburgite	dunite	ortho-pyroxenite	dunite	harzburgite	harzburgite	au hy gabbro	au gabbro	au hy gabbro	lherzolite	hornblendite	dunite	dunite	hb gabbro	au hb gabbro	au gabbro
Chemical Composition	SiO_2	39.50	40.60	43.80	39.40	42.30	38.80	44.00	41.40	46.20	40.30	44.30	42.50	41.50	46.90	48.80	54.50
	TiO_2	0.01	0.00	0.02	0.01	0.00	0.00	2.33	0.24	0.20	0.02	0.98	0.00	0.00	1.28	1.15	1.00
	Al_2O_3	0.76	0.47	1.26	0.56	0.54	0.49	14.40	16.90	19.20	1.55	12.00	0.34	0.26	16.30	15.00	15.20
	Fe_2O_3	8.28	7.46	5.56	7.46	6.46	7.94	8.24	5.08	3.46	7.44	7.69	7.34	6.82	4.69	6.55	8.15
	FeO	0.59	0.88	2.53	0.49	1.46	0.65	3.47	2.06	2.17	0.77	6.22	0.41	0.43	5.12	3.64	2.64
	MnO	0.13	0.13	0.14	0.12	0.13	0.09	0.26	0.13	0.12	0.10	0.48	0.11	0.05	0.23	0.20	0.20
	MgO	36.80	38.80	44.30	41.30	41.10	40.50	7.82	10.90	8.89	40.10	15.00	39.50	41.70	7.89	7.60	5.83
	CaO	0.81	0.37	2.12	0.63	0.94	0.38	12.60	15.20	12.00	0.93	9.91	0.36	0.31	13.80	9.31	4.26
	Na_2O	0.12	0.08	0.05	0.12	0.00	0.03	1.50	1.48	1.58	0.09	1.45	0.12	0.04	1.42	2.84	4.86
	K_2O	0.15	0.23	0.19	0.38	0.23	0.32	0.28	0.39	0.21	0.39	0.27	0.08	0.27	0.54	0.76	0.46
	P_2O_5	0.40	0.30	0.21	0.31	0.20	0.32	0.16	0.08	0.06	0.29	0.19	0.30	0.29	0.13	0.22	0.35
	Cr_2O_3	0.30	0.28	0.00	0.39	0.34	0.24	0.00	0.03	0.00	0.29	0.05	0.29	0.85	0.04	0.00	0.00
	NiO	0.23	0.23	0.00	0.24	0.24	0.59	0.00	0.01	0.00	0.20	0.02	0.26	0.35	0.01	0.00	0.00
	BaO	0.00	0.00	0.00	0.00	0.00	0.00	0.00	0.00	0.00	0.00	0.00	0.00	0.00	0.00	0.00	0.00
	L.O.I	12.20	11.00	0.40	9.60	7.00	10.50	1.10	2.10	2.00	9.10	2.10	9.90	9.00	0.90	2.00	3.20
	Total	100.00	100.83	100.58	101.01	100.94	100.85	96.16	96.00	96.09	101.57	100.66	101.51	101.87	99.25	98.07	100.65
C.I.P.W. Norm	q	0.00	0.00	0.00	0.00	0.00	0.00	2.42	0.00	0.31	0.00	0.00	0.00	0.00	0.00	2.78	7.76
	c	0.00	0.00	0.00	0.00	0.00	0.00	0.00	0.00	0.00	0.00	0.00	0.00	0.00	0.00	0.00	0.00
	or	0.89	1.36	1.12	2.25	1.36	1.89	1.65	2.30	1.24	2.30	1.60	0.47	1.42	3.19	4.49	2.72
	ab	1.02	0.68	0.42	0.76	0.00	0.25	12.69	12.52	12.95	0.76	12.27	1.02	0.00	12.02	24.03	41.12
	an	1.09	0.00	2.65	0.00	0.79	0.00	31.73	38.32	44.90	2.67	25.44	0.00	0.00	36.51	25.94	18.30
	ne	0.00	0.00	0.00	0.00	0.00	0.00	0.00	0.00	0.00	0.00	0.00	0.00	0.00	0.00	0.00	0.00
	di wo	0.13	0.00	2.71	0.46	1.07	0.00	12.41	15.27	5.95	0.02	9.39	0.00	0.00	12.99	7.86	0.23
	di en	0.10	0.00	2.14	0.36	0.85	0.00	10.73	13.19	4.96	0.02	5.50	0.00	0.00	7.03	6.79	0.20
	di fs	0.02	0.00	0.27	0.04	0.10	0.00	0.00	0.00	0.23	0.00	3.43	0.00	0.00	5.51	0.00	0.00
	hy fs	3.21	3.03	1.28	1.23	2.52	1.65	0.00	0.00	0.79	1.68	0.11	3.47	2.11	2.20	0.00	0.00
	hy en	21.13	22.32	10.08	10.44	20.72	13.66	8.75	0.00	17.18	13.04	0.17	28.62	21.93	2.81	12.14	14.32
	ol fo	49.35	52.02	68.76	64.52	56.62	61.05	0.00	0.00	0.00	60.84	22.20	48.85	57.41	6.88	0.00	0.00
	ol fs	8.26	7.80	9.66	8.38	7.59	8.14	0.00	0.00	0.00	8.66	15.25	6.52	6.10	5.94	0.00	0.00
	mt	0.00	0.00	0.00	0.00	0.00	0.00	5.28	6.35	5.02	0.00	0.00	0.00	0.00	0.00	9.05	6.26
	hm	0.00	0.00	0.00	0.00	0.00	0.00	4.60	0.70	0.00	0.00	0.00	0.00	0.00	0.00	0.31	3.83
	il	0.02	0.00	0.04	0.02	0.00	0.00	4.43	0.46	0.38	0.04	1.86	0.00	0.00	2.43	2.18	1.90
	ru	0.00	0.00	0.00	0.00	0.00	0.00	0.00	0.00	0.00	0.00	0.00	0.00	0.00	0.00	0.00	0.00
	ap	0.93	0.70	0.49	0.72	0.46	0.74	0.37	0.19	0.14	0.67	0.44	0.70	0.67	0.30	0.51	0.81
	cc	0.00	0.00	0.00	0.00	0.00	0.00	0.00	0.00	0.00	0.00	0.00	0.00	0.00	0.00	0.00	0.00
	cr	0.44	0.41	0.00	0.57	0.50	0.35	0.00	0.04	0.00	0.43	0.07	0.43	1.25	0.06	0.00	0.00
	tr	0.72	0.72	0.00	0.75	0.75	1.85	0.00	0.00	0.00	0.63	0.06	0.82	1.10	0.03	0.00	0.00
	sp	0.00	0.12	0.00	0.00	0.00	0.13	0.00	0.00	0.00	0.00	0.00	0.08	0.00	0.00	0.00	0.00
	MgO	0.00	0.00	0.00	0.00	0.00	0.00	0.00	0.00	0.00	0.00	0.00	0.00	0.00	0.00	0.00	0.00
	FeO	0.00	0.00	0.00	0.00	0.00	0.00	0.00	0.00	0.00	0.00	0.00	0.00	0.00	0.00	0.00	0.00
	lc	0.00	0.00	0.00	0.00	0.00	0.00	0.00	0.00	0.00	0.00	0.00	0.00	0.00	0.00	0.00	0.00
	Total	87.31	89.16	99.62	86.62	93.33	89.71	95.06	89.34	94.05	91.76	97.79	90.98	91.99	97.90	96.08	97.45
S.I.*		80.10	81.77	84.17	83.02	83.45	81.92	36.70	54.75	54.51	82.19	48.97	83.25	84.65	40.13	35.53	26.57
MgOx100 /(FeO+MgO)		98.42	97.78	94.60	98.83	96.57	98.42	69.26	84.10	80.38	98.12	70.69	98.97	98.98	60.65	67.62	68.83

* S.I. = MgOx100/(MgO+Fe_2O_3+FeO+Na_2O+K_2O)

Table I-4 Chemical Composition and C.I.P.W. Norm (2)

	Rock Type	Ultramafic Complex																
		Bongabong Body						Ogos Body						Other Bodies				
	Location	Samagui R.	Samagui R.	Banus R.	Banus R.	Rosanna R.	Rosanna R.	Ogos R.	Ogos R.	Ogos R.	Ogos R.	Aglubang R.	Alagag R.	Maril	San Vicente	Binuangan R.	Balete R.	Balete R.
	Sample No.	KR2-082	KR2-085	TR2-131	TR2-132	YR2-080	YR2-081	KR2-102	KR2-104	KR2-108	KR2-110	SR2-155	YR2-115	KR2-067	TR2-064	YR2-043	KR2-094	KR2-091
	Rock Name	harzburgite	ortho-pyroxenite	lherzolite	dunite	harzburgite	dunite	harzburgite	dunite	dunite	harzburgite	dunite	dunite	harzburgite	harzburgite	dunite	harzburgite	au hy gabbro
Chemical Composition	SiO_2	41.00	43.10	37.20	34.80	43.30	34.20	45.10	40.00	37.50	42.50	38.60	36.10	39.80	40.30	40.10	41.00	49.30
	TiO_2	0.01	0.00	0.01	0.00	0.01	0.00	0.07	0.00	0.00	0.00	0.00	0.00	0.00	0.02	0.00	0.02	0.25
	Al_2O_3	1.33	0.41	0.85	0.20	1.16	0.14	1.71	0.24	0.20	1.07	0.69	0.33	1.06	1.42	0.72	1.93	17.50
	Fe_2O_3	7.14	5.03	6.71	7.39	4.70	5.93	5.66	6.91	6.61	5.51	6.56	4.75	7.98	7.46	5.22	6.95	4.02
	FeO	0.76	2.59	0.66	0.75	2.33	1.03	1.12	0.88	1.52	2.32	0.79	0.85	0.80	0.49	0.49	0.63	1.12
	MnO	0.14	0.13	0.11	0.12	0.12	0.10	0.13	0.11	0.12	0.13	0.11	0.11	0.11	0.12	0.10	0.12	0.15
	MgO	40.70	47.70	40.00	44.30	43.30	47.90	33.10	43.00	46.20	42.70	41.90	46.50	42.30	38.10	40.60	41.50	10.10
	CaO	0.30	0.58	1.61	0.41	1.43	0.31	9.78	0.60	0.45	1.28	1.01	0.36	0.27	1.07	0.51	0.81	12.40
	Na_2O	0.07	0.10	0.09	0.12	0.08	0.09	0.22	0.11	0.02	0.06	0.11	0.18	0.03	0.06	0.15	0.22	1.73
	K_2O	0.05	0.05	0.15	0.05	0.20	0.04	0.04	0.01	0.04	0.00	0.14	0.09	0.07	0.04	0.07	0.07	0.14
	P_2O_5	0.32	0.18	0.27	0.33	0.22	0.27	0.17	0.26	0.24	0.22	0.31	0.24	0.30	0.28	0.26	0.29	0.05
	Cr_2O_3	0.32	0.48	0.20	0.22	0.33	0.27	0.34	0.21	0.56	0.27	0.35	0.44	0.31	0.33	0.00	0.35	0.00
	NiO	0.22	0.25	0.21	0.24	0.22	0.26	0.13	0.22	0.24	0.21	0.23	0.01	0.23	0.22	0.00	0.20	0.00
	BaO	0.00	0.00	0.00	0.00	0.00	0.00	0.00	0.00	0.00	0.00	0.00	0.00	0.00	0.00	0.00	0.00	0.00
	L.O.I	10.00	1.00	11.50	9.70	2.80	9.90	3.80	12.00	6.20	4.00	9.90	10.00	9.50	10.00	7.10	7.90	2.80
	Total	102.36	101.60	99.57	98.63	100.20	100.44	101.37	104.55	99.90	100.27	100.70	99.96	102.76	99.91	95.32	101.99	99.56
C.I.P.W. Norm	q	0.00	0.00	0.00	0.00	0.00	0.00	0.00	0.00	0.00	0.00	0.00	0.00	0.00	0.00	0.00	0.00	1.88
	c	0.00	0.00	0.00	0.00	0.00	0.00	0.00	0.00	0.00	0.00	0.00	0.00	0.00	0.00	0.00	0.00	0.00
	or	0.30	0.30	0.89	0.00	1.18	0.00	0.24	0.06	0.00	0.00	0.83	0.00	0.41	0.24	0.41	0.41	0.83
	ab	0.59	0.85	0.76	0.00	0.68	0.00	1.86	0.93	0.00	0.51	0.93	0.00	0.25	0.51	1.27	1.86	14.64
	an	0.00	0.52	1.47	0.00	2.22	0.00	3.56	0.13	0.34	2.65	0.98	0.00	0.00	3.48	0.83	2.12	39.57
	ne	0.00	0.00	0.00	0.41	0.00	0.27	0.00	0.00	0.09	0.00	0.00	0.65	0.00	0.00	0.00	0.00	0.00
	di wo	0.00	0.49	1.98	0.00	1.44	0.00	18.31	0.48	0.14	0.94	0.84	0.09	0.00	0.00	0.00	0.00	9.03
	di en	0.00	0.40	1.58	0.00	1.15	0.00	14.39	0.38	0.11	0.75	0.67	0.07	0.00	0.00	0.00	0.00	7.80
	di fs	0.00	0.04	0.18	0.00	0.12	0.00	1.88	0.04	0.01	0.09	0.07	0.01	0.00	0.00	0.00	0.00	0.00
	hy fs	2.86	1.08	0.53	0.00	1.66	0.00	0.32	1.43	0.00	2.03	0.85	0.00	1.99	2.80	1.84	1.81	0.00
	hy en	23.17	10.64	4.53	0.00	16.02	0.00	2.42	12.43	0.00	17.07	7.80	0.00	15.08	21.54	19.16	15.73	17.36
	ol fo	54.00	75.52	65.54	74.05	63.54	74.28	45.99	66.07	80.13	62.04	67.20	78.14	62.62	51.41	57.37	60.92	0.00
	ol fs	7.35	8.41	8.39	9.35	7.26	7.27	6.63	8.35	9.67	8.12	8.07	6.72	9.10	7.37	6.08	7.73	0.00
	mt	0.00	0.00	0.00	0.00	0.00	0.00	0.00	0.00	0.00	0.00	0.00	0.00	0.00	0.00	0.00	0.00	3.37
	hm	0.00	0.00	0.00	0.00	0.00	0.00	0.00	0.00	0.00	0.00	0.00	0.00	0.00	0.00	0.00	0.00	1.69
	il	0.02	0.00	0.02	0.00	0.02	0.00	0.13	0.00	0.00	0.00	0.00	0.00	0.00	0.04	0.00	0.04	0.47
	ru	0.00	0.00	0.00	0.00	0.00	0.00	0.00	0.00	0.00	0.00	0.00	0.00	0.00	0.00	0.00	0.00	0.00
	ap	0.74	0.42	0.63	0.76	0.51	0.63	0.39	0.60	0.56	0.51	0.72	0.56	0.70	0.65	0.60	0.67	0.12
	cc	0.00	0.00	0.00	0.00	0.00	0.00	0.00	0.00	0.00	0.00	0.00	0.00	0.00	0.00	0.00	0.00	0.00
	cr	0.47	0.71	0.29	0.32	0.49	0.40	0.50	0.31	0.82	0.40	0.52	0.65	0.46	0.49	0.00	0.52	0.00
	tr	0.69	0.78	0.66	0.75	0.69	0.82	0.41	0.69	0.75	0.66	0.72	0.03	0.72	0.69	0.00	0.63	0.00
	sp	1.62	0.00	0.00	0.00	0.00	0.00	0.00	0.00	0.00	0.00	0.00	0.00	1.30	0.00	0.13	1.00	0.00
	MgO	0.00	0.00	0.00	1.88	0.00	5.34	0.00	0.00	0.25	0.00	0.00	1.70	0.00	0.00	0.00	0.00	0.00
	FeO	0.00	0.00	0.00	0.29	0.00	0.64	0.00	0.00	0.04	0.00	0.00	0.18	0.00	0.00	0.00	0.00	0.00
	lc	0.00	0.00	0.00	0.23	0.00	0.19	0.00	0.00	0.19	0.00	0.00	0.42	0.00	0.00	0.00	0.00	0.00
	Total	91.81	100.16	87.45	88.04	96.98	89.84	97.03	91.90	93.10	95.77	90.20	89.22	92.63	89.22	87.69	93.44	95.76
S.I.*		83.54	85.99	84.02	84.20	85.56	87.11	82.46	84.46	84.94	84.40	84.65	88.79	82.65	82.56	87.26	84.06	59.03
MgOx100/(FeO+MgO)		98.17	94.85	98.38	98.34	94.89	97.89	96.73	97.99	96.81	94.85	98.15	98.20	98.14	98.73	98.81	98.50	90.02

* S.I. = Mgox100/($MgO+Fe_2O_3+FeO+Na_2O+K_2O$)

Table I-4 Chemical Composition and C.I.P.W. Norm (3)

Rock Type		Ultramafic Complex			Lumintao Formation						Mansalay F.	Intrusive Rocks		Halcon Metamorphics				
		Other Bodies			Volcanic Rocks			Associated Intrusive Rocks			Volcanic Rocks	Acidic to Intermediate Rocks						
Location		Balete R.	Maril	San Vicente	Lumintao R.	Lumintao R.	Igsoso	Pintin R.	Liwliw	Lumintao R.	San Vicente	Sinambalan	Sinanbalan	Ogos R.	Amnay R.	Puerto Galera	Paluan R.	Alag R.
Sample No.		TR2-151	KR2-068	KR2-071	KR2-009	KR2-014	KR2-073	KR2-029	KR2-074	KR2-017	TR2-069	TR2-107	TR2-111	KR2-112	TR2-046	TR2-161	YR2-039	FR2-073
Rock Name		hb gabbro	diorite porphyry	trondhjemite	basalt	basalt	basalt	dolerite	dolerite	gabbro	basalt	diorite porphyry	quartz porphyry	green schist	amphibolite	mica schist	green schist	mica schist
Chemical Composition	SiO_2	43.40	60.60	68.90	48.00	48.80	50.00	50.80	47.20	45.50	46.30	48.60	61.10	47.10	47.60	71.30	57.60	57.30
	TiO_2	0.86	0.73	0.15	0.98	1.10	0.80	1.29	0.55	1.05	1.19	1.09	0.58	1.48	1.99	0.68	0.60	0.69
	Al_2O_3	14.20	16.30	12.30	15.60	14.90	15.20	14.90	14.10	16.50	15.60	17.10	15.60	14.10	16.90	14.20	13.50	16.30
	Fe_2O_3	6.25	2.03	1.36	7.91	6.94	7.15	8.59	5.36	6.35	6.65	7.08	4.30	7.44	7.74	2.42	5.55	5.75
	FeO	2.36	0.88	0.10	2.67	3.23	2.13	2.27	3.16	3.17	1.87	2.39	0.92	2.64	3.08	0.32	2.54	0.46
	MnO	0.16	0.05	0.01	0.18	0.18	0.17	0.18	0.19	0.18	0.18	0.13	0.08	0.21	0.39	0.00	0.23	0.09
	MgO	10.10	3.67	0.43	5.85	6.33	6.99	4.95	8.16	11.20	7.92	4.26	2.56	7.96	6.57	0.58	5.98	2.46
	CaO	9.72	4.81	4.25	9.91	9.93	9.63	8.43	14.40	8.16	7.83	7.20	2.18	12.00	8.22	0.31	2.85	2.22
	Na_2O	2.99	6.71	4.48	2.64	2.77	3.50	4.69	0.49	2.72	2.66	2.52	3.92	2.30	2.87	0.48	2.73	3.52
	K_2O	0.19	0.20	0.10	0.72	0.46	0.18	0.27	0.15	0.35	2.14	2.45	3.19	0.18	1.43	3.01	0.14	3.44
	P_2O_5	0.11	0.10	0.07	0.25	0.30	0.29	0.35	0.06	0.34	0.36	0.75	0.32	0.37	0.35	0.09	0.29	0.41
	Cr_2O_3	0.00	0.00	0.00	0.00	0.00	0.00	0.00	0.00	0.00	0.00	0.00	0.00	0.00	0.00	0.00	0.00	0.00
	NiO	0.00	0.00	0.00	0.00	0.00	0.00	0.00	0.00	0.00	0.00	0.00	0.00	0.00	0.00	0.00	0.00	0.00
	BaO	0.00	0.00	0.00	0.00	0.00	0.00	0.00	0.00	0.00	0.00	0.00	0.00	0.00	0.00	0.00	0.00	0.00
	L.O.I	7.00	1.60	1.90	3.10	2.50	4.10	2.20	2.10	3.90	4.40	2.00	3.10	2.10	1.80	3.70	5.10	2.80
	Total	97.34	97.68	94.05	97.81	97.44	100.14	98.92	95.92	99.42	97.10	95.57	97.85	97.88	98.94	97.09	97.11	95.44
C.I.P.W. Norm	q	0.00	7.35	34.52	4.73	5.47	3.17	2.51	8.16	0.00	0.00	5.49	18.50	2.87	1.06	55.71	26.98	16.39
	c	0.00	0.00	0.00	0.00	0.00	0.00	0.00	0.00	0.00	0.00	0.00	2.50	0.00	0.00	9.80	4.37	3.73
	or	1.12	1.18	0.59	4.25	2.72	1.06	1.60	0.89	2.07	12.65	14.48	18.85	1.06	8.45	17.79	0.83	20.33
	ab	24.62	56.78	37.91	22.34	23.44	29.62	39.69	4.15	23.02	22.51	21.32	33.17	19.46	24.29	4.06	23.10	29.79
	an	24.76	13.77	13.16	28.59	26.86	25.23	18.81	35.83	31.78	24.31	28.11	8.72	27.62	29.01	0.95	12.24	8.33
	ne	0.37	0.00	0.00	0.00	0.00	0.00	0.00	0.00	0.00	0.00	0.00	0.00	0.00	0.00	0.00	0.00	0.00
	di wo	9.49	3.94	1.24	7.91	8.53	8.62	8.66	14.70	2.71	5.09	1.13	0.00	12.32	3.96	0.00	0.00	0.00
	di en	8.21	3.41	1.07	6.83	7.38	7.45	7.48	12.33	2.34	4.40	0.98	0.00	10.64	3.42	0.00	0.00	0.00
	di fs	0.00	0.00	0.00	0.00	0.00	0.00	0.00	0.50	0.00	0.00	0.00	0.00	0.00	0.00	0.00	0.00	0.00
	hy fs	0.00	0.00	0.00	0.00	0.00	0.00	0.00	0.32	0.00	0.00	0.00	0.00	0.00	0.00	0.00	0.00	0.00
	hy en	0.00	5.73	0.00	7.74	8.39	9.96	4.85	8.00	13.92	7.64	9.63	6.38	9.18	12.94	1.44	14.89	6.13
	ol fo	11.88	0.00	0.00	0.00	0.00	0.00	0.00	0.00	8.16	5.39	0.00	0.00	0.00	0.00	0.00	0.00	0.00
	ol fs	0.00	0.00	0.00	0.00	0.00	0.00	0.00	0.00	0.00	0.00	0.00	0.00	0.00	0.00	0.00	0.00	0.00
	mt	5.64	0.88	0.00	6.35	7.78	5.10	4.16	7.77	7.76	3.17	4.97	1.55	4.90	5.43	0.00	7.20	0.00
	hm	2.36	1.42	1.36	3.53	1.57	3.63	5.72	0.00	1.00	4.47	3.65	3.23	4.06	3.99	2.42	0.59	5.75
	il	1.63	1.39	0.23	1.86	2.11	1.52	2.45	1.04	1.99	2.26	2.07	1.10	2.81	3.78	0.68	1.14	1.16
	ru	0.00	0.00	0.00	0.00	0.00	0.00	0.00	0.00	0.00	0.00	0.00	0.00	0.00	0.00	0.32	0.00	0.08
	ap	0.25	0.23	0.16	0.58	0.70	0.67	0.81	0.14	0.79	0.83	1.74	0.74	0.86	0.81	0.21	0.67	0.95
	cc	0.00	0.00	0.00	0.00	0.00	0.00	0.00	0.00	0.00	0.00	0.00	0.00	0.00	0.00	0.00	0.00	0.00
	cr	0.00	0.00	0.00	0.00	0.00	0.00	0.00	0.00	0.00	0.00	0.00	0.00	0.00	0.00	0.00	0.00	0.00
	tr	0.00	0.00	0.00	0.00	0.00	0.00	0.00	0.00	0.00	0.00	0.00	0.00	0.00	0.00	0.00	0.00	0.00
	sp	0.00	0.00	0.00	0.00	0.00	0.00	0.00	0.00	0.00	0.00	0.00	0.00	0.00	0.00	0.00	0.00	0.00
	MgO	0.00	0.00	0.00	0.00	0.00	0.00	0.00	0.00	0.00	0.00	0.00	0.00	0.00	0.00	0.00	0.00	0.00
	FeO	0.00	0.00	0.00	0.00	0.00	0.00	0.00	0.00	0.00	0.00	0.00	0.00	0.00	0.00	0.00	0.00	0.00
	lc	0.00	0.00	0.00	0.00	0.00	0.00	0.00	0.00	0.00	0.00	0.00	0.00	0.00	0.00	0.00	0.00	0.00
	Total	90.33	96.08	90.24	94.71	94.95	96.03	96.74	93.83	95.54	92.72	93.57	94.74	95.78	97.14	93.38	92.01	92.64
S.I. *		46.14	27.21	6.65	29.56	32.08	35.04	23.83	47.11	47.08	37.29	22.78	17.19	38.79	30.29	8.52	35.30	15.74
MgOx100 /(FeO+Mg)		81.06	80.66	81.13	68.66	66.21	76.64	68.56	72.08	77.94	80.90	64.06	73.56	75.09	68.08	64.44	70.19	84.25

* S.I. = $MgO \times 100/(MgO+Fe_2O_3+FeO+Na_2O+K_2O)$

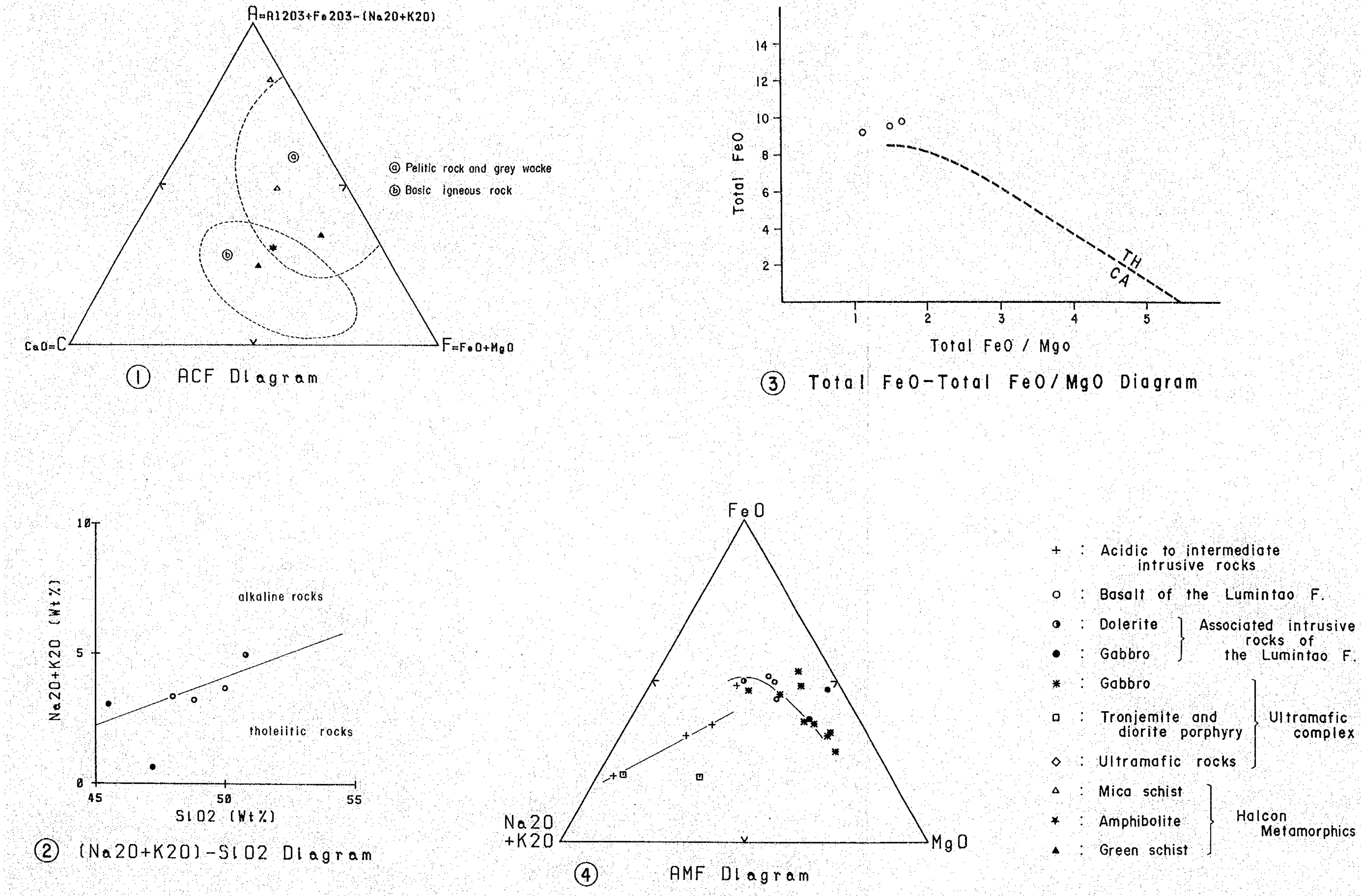

Fig. I-9 Diagrams of Chemical Composition (1)

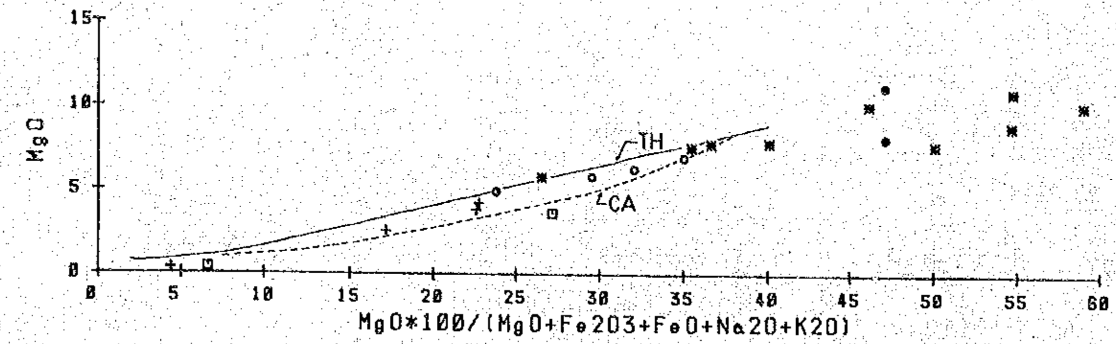

⑤ MgO-MgO*100/(MgO+Fe2O3+FeO+Na2O+K2O) Diagram

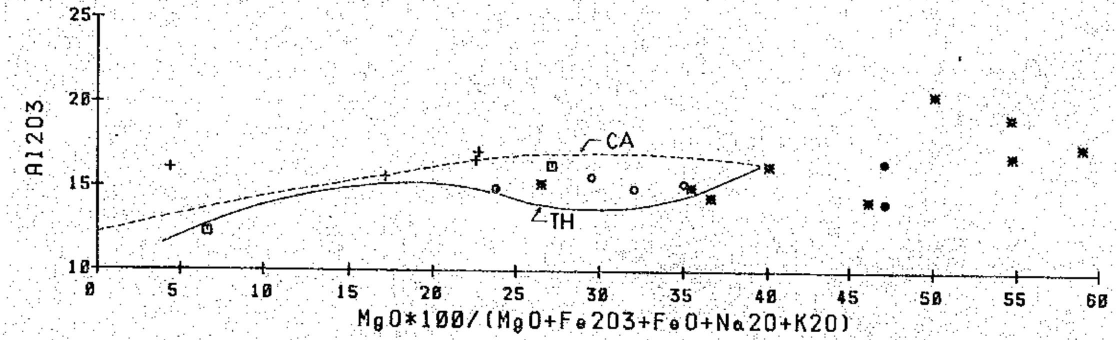

⑥ Al2O3-MgO*100/(MgO+Fe2O3+FeO+Na2O+K2O) Diagram

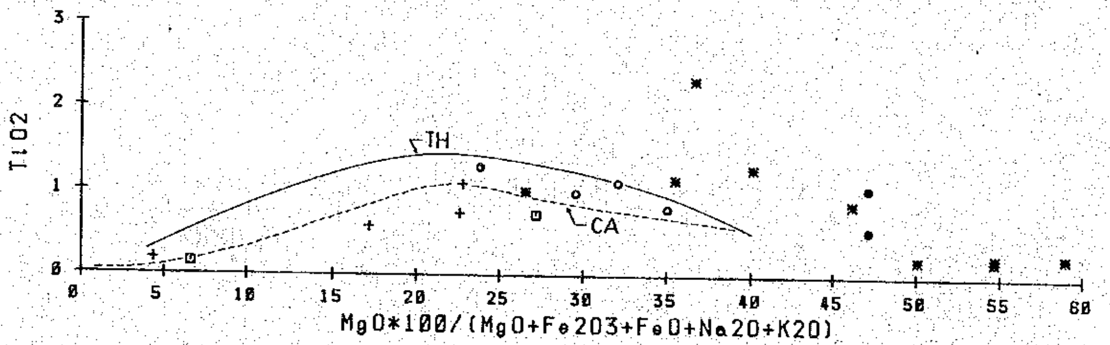

⑦ TiO2-MgO*100/(MgO+Fe2O3+FeO+Na2O+K2O) Diagram

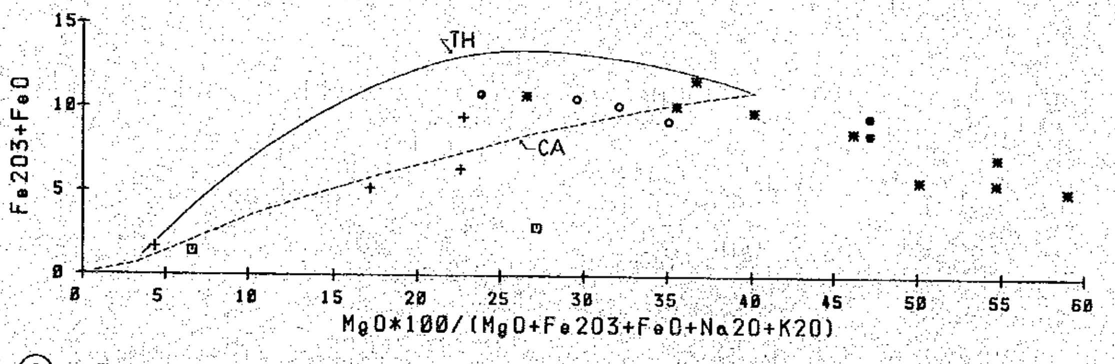

⑧ Fe2O3+FeO-MgO*100/(MgO+Fe2O3+FeO+Na2O+K2O) Diagram

Fig. I-9 Diagrams of Chemical Composition (2)

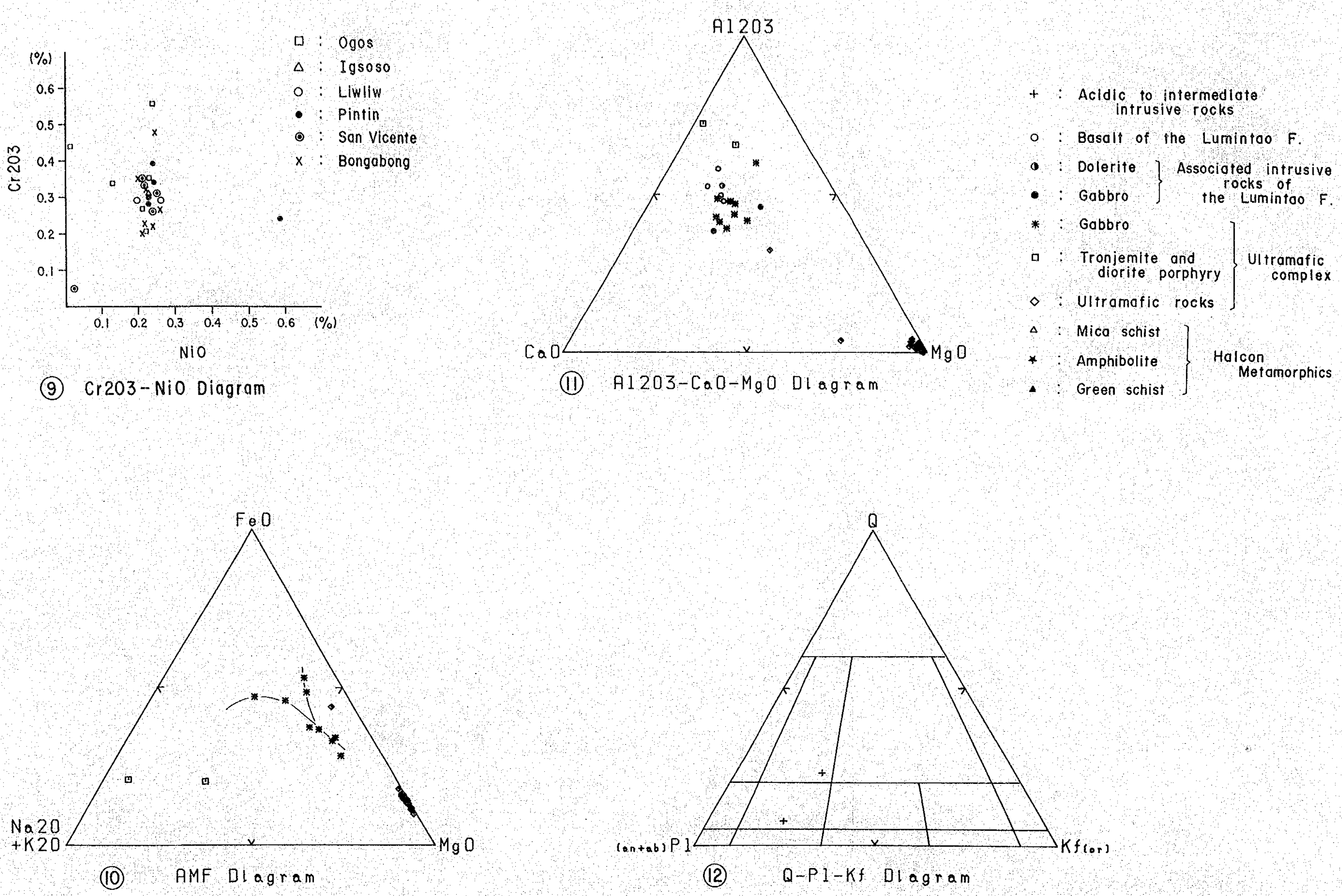

Fig. I-9 Diagrams of Chemical Composition (3) the field occurrences imply that gabbro might have crystallized in the shallow depth from the secondary magma reservoir, and that gabbroic pegmatite can be observed accompanied with gabbro.

1–5–3 Chemical Characteristics of the Ultramafic Complex

Twenty eight samples of the Ultramafic complex were analyzed.

(1) Ultramafic rocks

All the samples of the ultramafic rocks fall in SiO_2 range of 34.20 to 45.10 %. Each of the ultramafic complex body has similar Cr_2O_3 content and the average Cr_2O_3 content of all of the bodies is 0.33 % which is similar to that content of ultramafic rocks of other areas. Among the ultramafic complex bodies, Ogos body has the highest average Cr_2O_3 content of 0.36 %. Dunite has the highest Cr_2O_3 content of 0.35 % among the each rock types, on the other hand harzburgite and lherzolite have 0.31 % and 0.26 % respectively. In the accompanied rocks, orthopyroxinite (KR2–085) shows high content of 0.48 % Cr_2O_3 and hornblendite (KR2–077) shows fairly low of 0.05 %. A high Cr_2O_3 content of the sample KR2–085 may partly due to a occurrence of picotite in this sample.

The highest value of Cr_2O_3 content was obtained from dunite of the Ogos body in which the widest chromite deposit occurs, and these fact may suggest that a high Cr_2O_3 content of rocks can be considered as a high potentiality of the chromite deposit.

As for NiO content, each rock type has a similar value such as 0.25 %, 0.24 % and 0.21 % for harzburgite, lherzolite and dunite respectively. Orthopyroxenite has 0.25 % of NiO content, while hornblendite has quite low NiO value of 0.02 %. The average NiO content of the whole samples is 0.23 % and the Pintin body has the highest NiO content of 0.31 % among the bodies. There is no significant difference in the NiO content among the each body, consequently in the Cr_2O_3-NiO diagram (Fig. I–9-3 ⑨) the clear differences between each bodies can not be seen.

MgO x 100 / (MgO + Total FeO) ratios for all of the samples, ranging from 82 to 90 % with the highest value in the Bongabong body (Table I–4), fall in the field of the ultramafic rocks of the Alpine type.

Forsterite components of normative olivine for each sample fall in quite narrow range of 88 to 90 %, however it is necessary to analyze olivines for a critical discussion of an olivine.

In the AMF diagram (Fig. I–9-3 ⑩), all of the ultramafic rocks are seen in the small area except one sample of hornblendite which can be seen near the Fe corner. All of the samples are plotted around MgO apex of the MgO – CaO – Al_2O_3 diagram (Fig. I–9-3 ⑪), and it is correspond to the metamorphic peridotite field of Coleman's subdivision (1977).

(2) **Basic rock (gabbro)**

The gabbro of the ultramafic complex, having quite a wide range of SiO_2 content from 43.40 % to 54.57 %, show the differentiation trend of tholeiitic rock similar to that of basaltic rocks of Lumintao formation in AMF diagram (Fig. I–9-3 ⑩) and the solidification index vs. MgO, Al_2O_3, TiO_2 and Fe_2O_3 + FeO diagram (Fig. I–9-2 ⑤–⑧). These chemical characteristics probably suggest that these gabbro represent various stage of differentiation originated from the single parental magma.

The chemical similarities among these gabbro, basalt of the Lumintao formation, dolerite and gabbro related to the Lumintao formation, imply that they might have evolved from the similar parental magma and similar igneous processes.

1–5–4 Chemical Characteristics of Acidic to Intermediate Intrusive Rocks

The samples of granodiorite and quartz diorite exposed in the iron deposit region in the northern part, are selected for chemical analyses. TR2–107 and TR2–111, respectively, fall in the quartz monzodiorite field and granodiorite field in the normative Q–Pl–Kf diagram (Fig. I–9–3 ⑫). Addition to these samples, two samples analyzed in Phase I were also considered in the AMF diagram (Fig. I–4). The distribution of these samples in the diagram, lying on the one straight line which is correspond to the differential trend of plutonic rocks of calc-alkalic series, may suggest that these rocks are the products of differentiation of a single calc-aklaline magma.

1–6 Geological Structure and Geological History

1–6–1 Geological Structure

The survey area can be divided into five geotectonic zones: that is (I) Central life zone, (II) Paluan lift zone, (III) Mamburao basin, (IV) Southwestern basin and (V) Eastern basin (Fig. I–10).

The Central and the Paluan lift zones, which build the mountain range in Mindoro Island, are composed of Halcon metamorphics and are separated by Mamburao basin. The Mamburao, the Southwestern and the Eastern basins are filled by a series of Cenozoic sediments ranging from the Mamburao to the Socorro groups and form the low lands. Large-scale faults and ultramafic intrusion are found near the boundary between the lift zone and the basin.

It is considered based on the distribution of tectonic zones and the geological sections that the whole island shows a large anticlinal structure trending NW–SE. The following three systems of the structure can be recognized in the area.

1 NNW ~ NW–SE system

This system is the most remarkable direction as shwon by the elongation of Mindoro Island, accordingly the system is recognized in the whole area on the structures such as fault, fold, general strike of the sedimentary rocks and intrusive rocks.

The faults of this systems are represented by the Mindoro fault extending over 60 km and the Wasig fault extending over 50 km, both of which are eastside-slipped gravity faults, bordering the central lift zone from the Eastern basin. Besides these, the westside-slipped gravity fault with steep dip is located to the east of Sablayan and the faults diverged from the Mindoro fault and Wasig fault are distributed in a horsetail around the upper reaches of the Balete River.

As for folds of this system, the broad anticline has been formed in the Mansalay formation in the central portion and small-scale folds with an axial length of 2 – 10 km and a wave length of 1 – 2 km are formed in the Sablayan group, Bongabong group and Socorro group in the southern portion. The intrusive rocks trending NNW–SSE to NW–SE are recognized as the Bongabong body, Pintin body, Igsoso body and Balete bodies of Ultramafic complex, and some quartz dioritic dikes.

The movement for forming this system is considered to start after Cretaceous and continue until Pleistocene in which the movement was most active.

2 NE–SW system

This system can be found in the trend of fold and fault.

There are two types of fold which are old stage fold developing in the Baco group and new one developing in the Mamburao basin. The former shows a wave length of 1 – 5 km in the southeast and 10 km in the central part with a axial length of 3 – 10 km, and the latter is larger scale than the former, with a wave length of over 15 km and an axial length of over 30 km.

Faults of this system are represented by the Mamburao fault which is an eastside-slipped gravity fault with an extention of 25 km, bordering the Mamburao basin from the Paluan lift zone. In addition to this, the faults are encountered in the middle reaches of the Lumintao River, where the tectonic depression has been formed by faults of this system together with E–W and NW–SE systems.

The activity forming these structures presumed to take place first after the sedimentation of the Baco group, from late Jurassic to early Cretaceous time, and secondly after the sedimentation of the Sablayan group, from Pliocene to Pleistocene time.

3 WNW–ESE ~ E–W system

This system can be recognized as the faults distributed along the Mindoro fault, the elongation of the Ogos body and Liwliw body, and the small-scale folds formed in the Mansalay formation to the west of Sta. Cruz. In particular, this system is prominently recognized in the area around the Ogos body, Sta. Cruz and Mamburao.

The system may have been formed after the sedimentation of the Baco group and before the intrusion of Ultramafic complex, namely from late Jurassic to Creaceous time.

1–6–2 Geological History

In Phase I, the stratigraphic relationship between the Halcon metamorphics and the Baco group was inferred to be unconformable, and the Halcon metamorphics was regarded as the basement rocks of the area. In this phase, however, it is confirmed that there is the place where the Baco group conformably overlies the Halcon metamorphics. Consequently, Paleozoic rocks may not be exposed in Mindoro Island.

In Jurassic period, a large-scale subsidence took place and formed the sedimentary basin of the Baco group. The basin is characterized by different deposition, that is, deposition of thick sandstone and mudstone with some volcanic rocks in the earlier stage and deposition of thick basalt lava by vigorous igneous activity in the later stage.

From late Jurassic age an orogenic movement had taken place, and it is inferred that the movement was accompanied by metamorphism. By this movement the NE–SW trending folds were formed in the Baco group, furthermore the structure of NNW–SSE ~ NW–SE and WNW–ESE ~ E–W systems were formed between blocks with different movement, which led to the intrusion of Ultramafic complex.

During Tertiary period, marine transgression and retrogression were repeated and the netric Mamburao, Sablayan and Bongabong groups were deposited. The differential uplifting in this period was so distinct that the sedimentary basin split into two (east and west sides) across the central portion, resulting in some differences in rock facies deposited. That is, the west side is characterized by limestone and conglomerate with few volcanic rocks, on the contrary, the east side characterized by tuff, tuffaceous mudstone to siltstone and sandstone. During Eocene and Oligocene age, the intrusion of acidic to intermediate plutonic rocks had taken place as the succession of orogenic movement, and iron ore deposits were formed.

Contrary to the Tertiary system stated above, the sedimentary basin of the Socorro group deposited chiefly in Quaternary was almost continental except that of reef limestone.

The structure of NNW–SSE system formed by uplifting which started from late Jurassic, had become more clear during Pliocene and Pleistocene period, and appeared as the Mindoro fault, the Wasig fault and some foldings. With almost he same time, a synclinal structure with a NE system and the Mamburao fault were formed in Mamburao area.

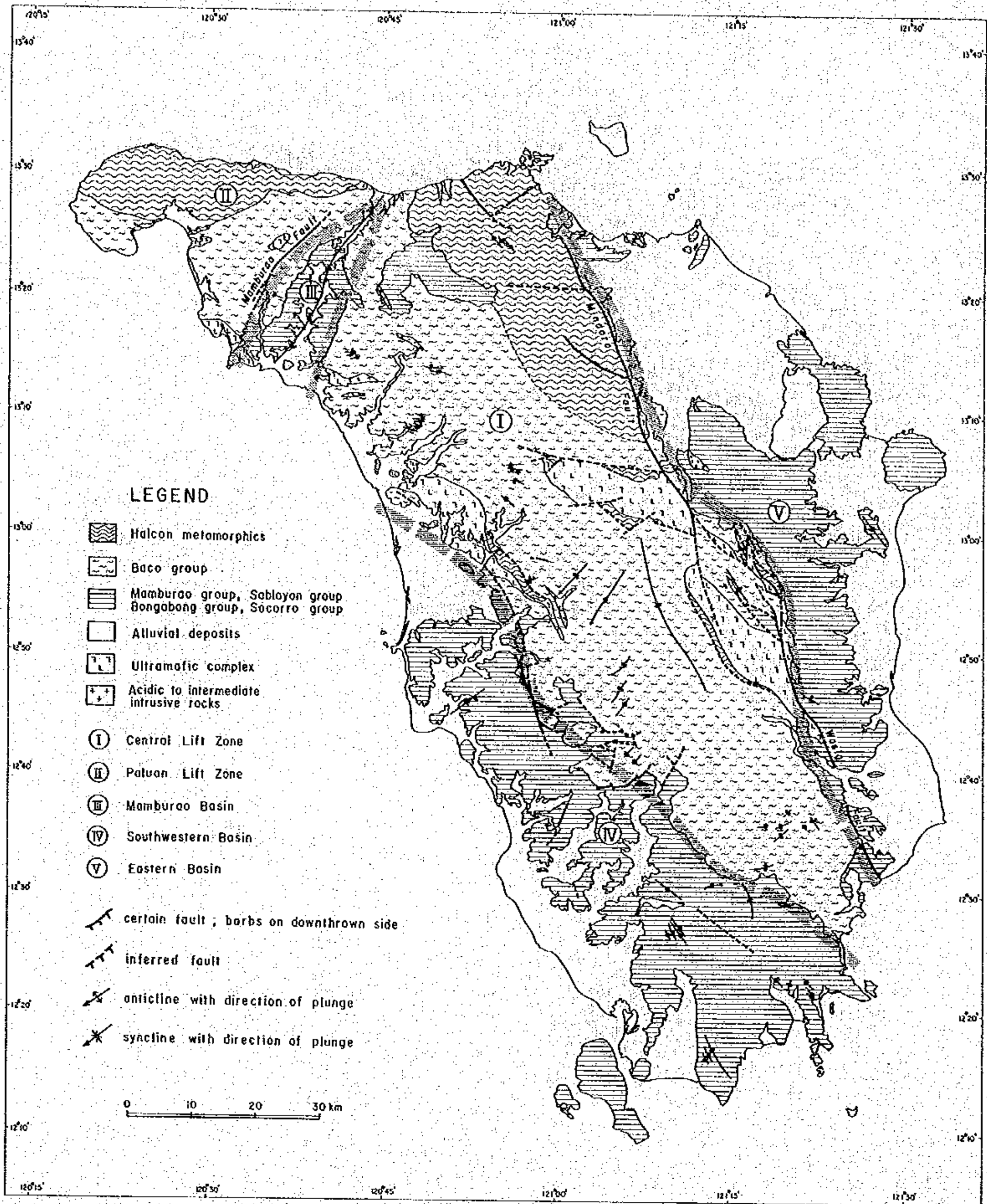

Fig. I-10 Tectonic Map of the Survey Area

Chapter 2 Ore Deposits

2–1 General Remarks

Various kinds of showings have been known in Mindoro Island, and 53 showings were listed in the table of ore deposits in the Phase I report, based on the existing data and the geological reconnaissance survey results. In this phase, a check survey was conducted on these showings and made clear the occurrence of ore deposits of chromium, iron and copper, etc. and several new showings were found out.

Table I–5 shows the numbers of showings listed, checked in Phase I and II and newly found out in Phase II by ore kind.

Table I-5 Number of Listed, Checked and New Showings

Commodity	Listed in Phase I	Checked in Phases I&II	Newly found in Phase II
Gold	2 places	2 places	0 places
Copper	7	3	1
Nickel-Chrome	8	5	4
Iron	15	6	3
Barite	4	3	0
Feldspar	1	0	0
Talc	2	0	0
Gypsum	2	0	1
Silica	6	6	0
Marble	2	2	0
Jade	1	1	0
Coal	3	3	1
Total	53	31	10

2–2 Details of Each Ore Deposit

The details of ore deposits or showings checked this time is as follows, among which chromium, copper and iron deposits seem to be promising.

2–2–1 Chromium-Nickel Deposits

The deposits are accompanied with the Ultramafic complex, and occurrences of ore deposits such as Ogos and Banus in Mindoro Oriental, and Paluan, Igsoso, San Vicente, Liwliw, Paragpagan

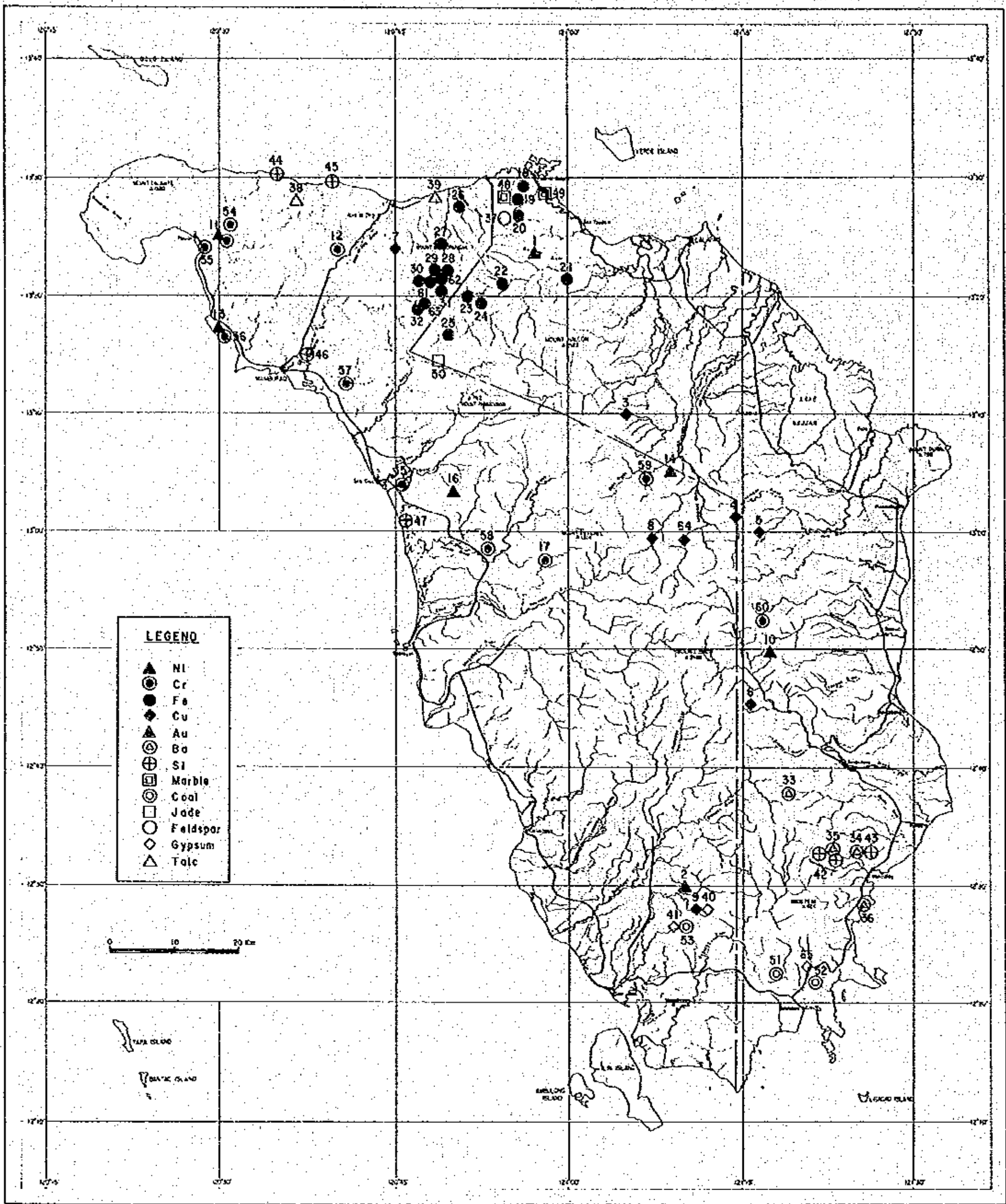

Fig. I-11 Location Map of Mineral Showings

gan and Pintin in Mindoro Occidental became clear.

(A) Ogos chromite deposit (No. 59 in Inventory Table)

The deposit is found in a branch in the midstream of the Ogos River, the western tributary of the Megasowagtubic River, 10 km south–southwest of Villacervesa. It was discovered by the Phase II survey. It takes whole one day to foot on reach the site along the Ogos River when the water level is low.

The Ultramafic complex body exposed here has a size of 22 km in E–W direction and 6 to 8 km in N–S, mainly consisting of dunite > harzburgite, lherzolite. A layered structure is notable.

The outcorp of chromite ore deposit is located almost in the center of the complex body, occurring in dunite near the boundary between dunite and harzburgite. Fig. I–12 shows a sketch of the outcrop on the gentle slope (about 20°) on the northern bank of the branch. The ore shows a banding structure which grades from disseminated near the wall to densely spotted in the center, tending to get coarser in the grain size. Chromite grains are disseminated in the wall rock of dunite and gradually change into the densely spotted ore on the footwall side (southern side), while the hanging wall side is bordered by a small fault. The width of the ore body is about 5 m, striking N80°E and dipping 70°N. Its extension is unclear, because it is covered by terrace deposit on both sides.

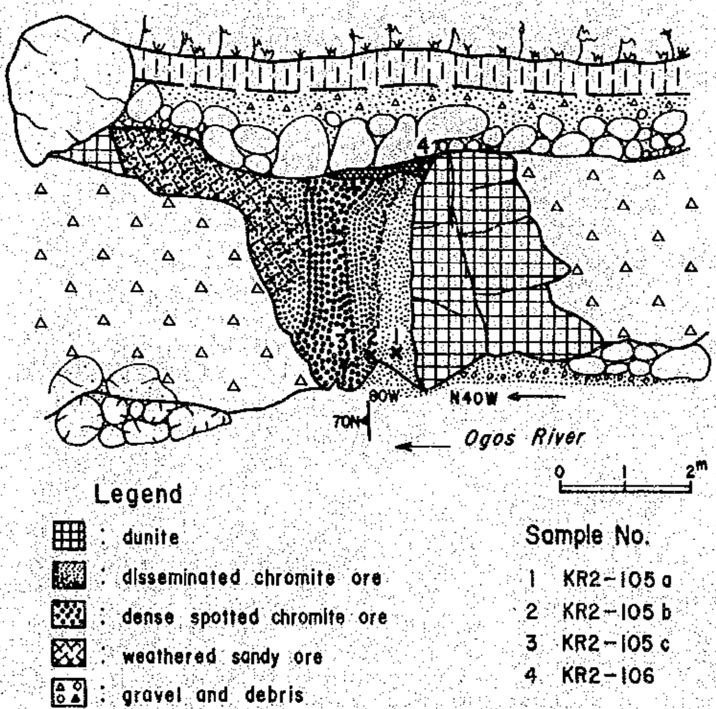

Fig. I-12 Ogos Chromite Deposit

The ore is relatively compact and hard. Microscopically, chromite occurs in an euhedral but a slightly rounded form, 0.5 to 1.5 mm in size.

The grain size in the center part is somewhat coarser, 0.3 mm to 2.0 mm in size. Mechanical cracks occur throughout the field, and a small amount of pyrite grains of 0.03 to 0.06 mm are included.

Analytical results of the ores are shown below.

Sample No.	Cr_2O_3 %	Fe %	SiO_2 %	Al_2O_3 %	MgO %	Ni %	Co ppm
KR2–105a (marginal part)	29.99	14.14	9.80	7.75	14.32	0.10	68
KR2–105b (middle part)	31.39	12.29	9.12	7.80	13.83	0.09	50
KR2–105c (central part)	28.28	10.86	6.22	7.55	11.82	0.07	26
KR2–106 (weathered part)	37.05	13.29	5.58	9.09	6.20	0.04	24

(B) Banus chromite deposit (No. 60)

The deposit is situated at the place of 580 meters above sea level, in the southern branch of the upper stream of the Banus River. It was newly found out this time like Ogos deposit. In the dry season, it can be reached by going up the river on foot about 3.5 km from the end of the logging road.

The ultramafic body related to the ore deposit has a width of about 6 km in this area and extends more than 30 km in the direction of NW–SE. The rocks along the Banus River consists of harzburgite > dunite > lherzolite, all of them are intruded by small-scale hypersthene-augite gabbro and augite gabbro. A layered structure is partly observed in the rocks.

The chromite deposit is emplaced in lherzolite near the boundary between lherzolite and dunite. The ore is found in a shear zone of 1 m wide, striking N20°E and dipping 20°S. It is composed of lenticular, massive, densely spotted and disseminated ores of 0.10 to 0.15 m thick, totaling more than 0.50 m (Fig. I–13).

Under the microscope, the massive ore mostly consists of anhedral grains of chromite, and coarse-grained euhedral crystals are also observed in a small amount. Some crystals are broken into 0.05 to 1.0 mm in size (0.2 mm in average), showing a cataclastic texture. Coarse euhedral crystals have a rounded form with a brecciated margin which is made by rotation owing to shearing. In a small amount of pyrite and magentite grains, less than 0.02 mm in size, are included as paragenetic minerals.

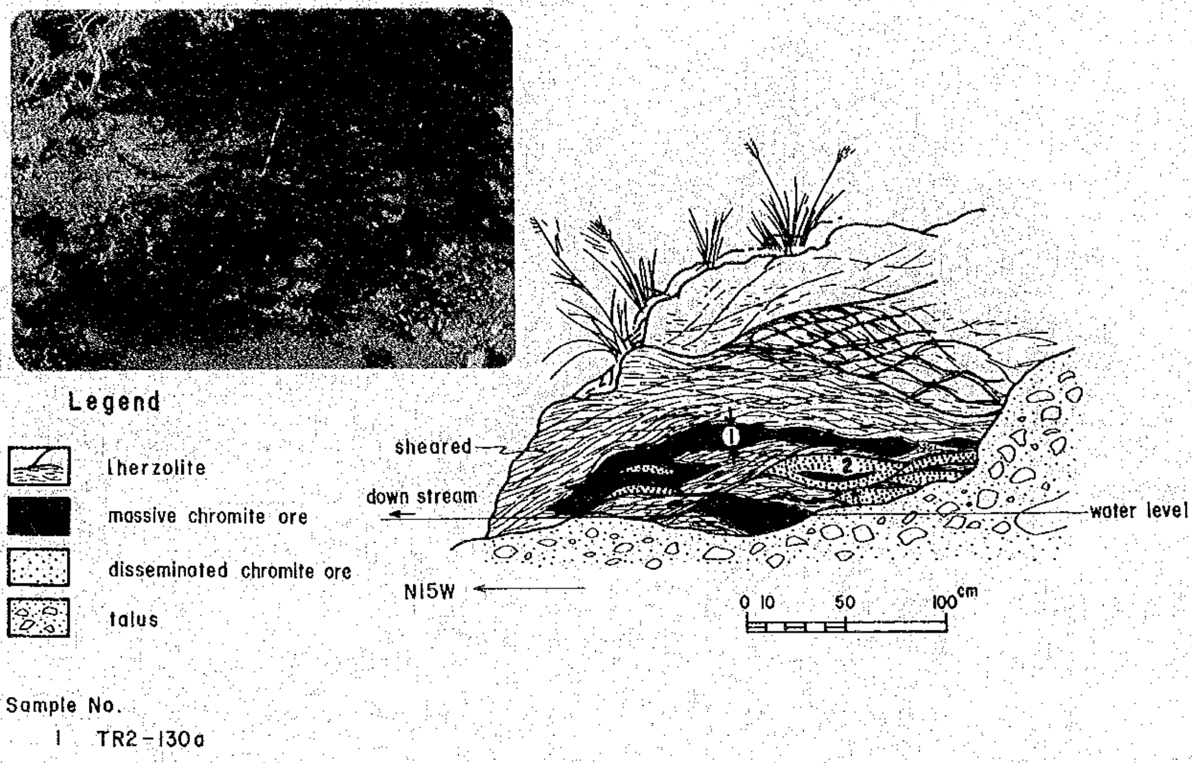

Fig. I-13 Banus Chromite Deposit

Chemical analysis:

Sample No.	Thick-ness	Cr_2O_3 %	Fe %	SiO_2 %	Al_2O_3 %	MgO %	Ni %	Co ppm
TR2 -130a (massive ore)	0.10m	34.50	12.43	11.80	6.42	19.56	0.05	46
TR2–130b (disseminated ore)	0.20	27.08	8.71	19.08	3.97	31.63	0.13	23

(C) Igsoso Chromite Deposit (No. 56)

The deposit is situated on the hill, 11 km northwest of Mamburao, and it will take 20 minutes on foot to get here from the Mamburao – Paluan highway. (Fig. I–14).

The Ultramafic complex body of the area is distributed on a small scale, 10 km in the NW–SE direction with a width of 2 to 3 km, and consists of dunite, harzhurgite and pyroxenite. They have a layered structure, and the central part of the complex is intruded by augite gabbro, augite-hornblende gabbro and a small-scale microdiorite.

The chromite deposit is emplaced in dunite, showing a bedded to disseminated form. Eleven ore layers of 0.01 to 0.20 m wide are observed in a width of 1.0 to 1.5 m. Generally dunite is dark greenish gray in color, but the very close part to the ore (about 3 m wide) is altered to yellow in color.

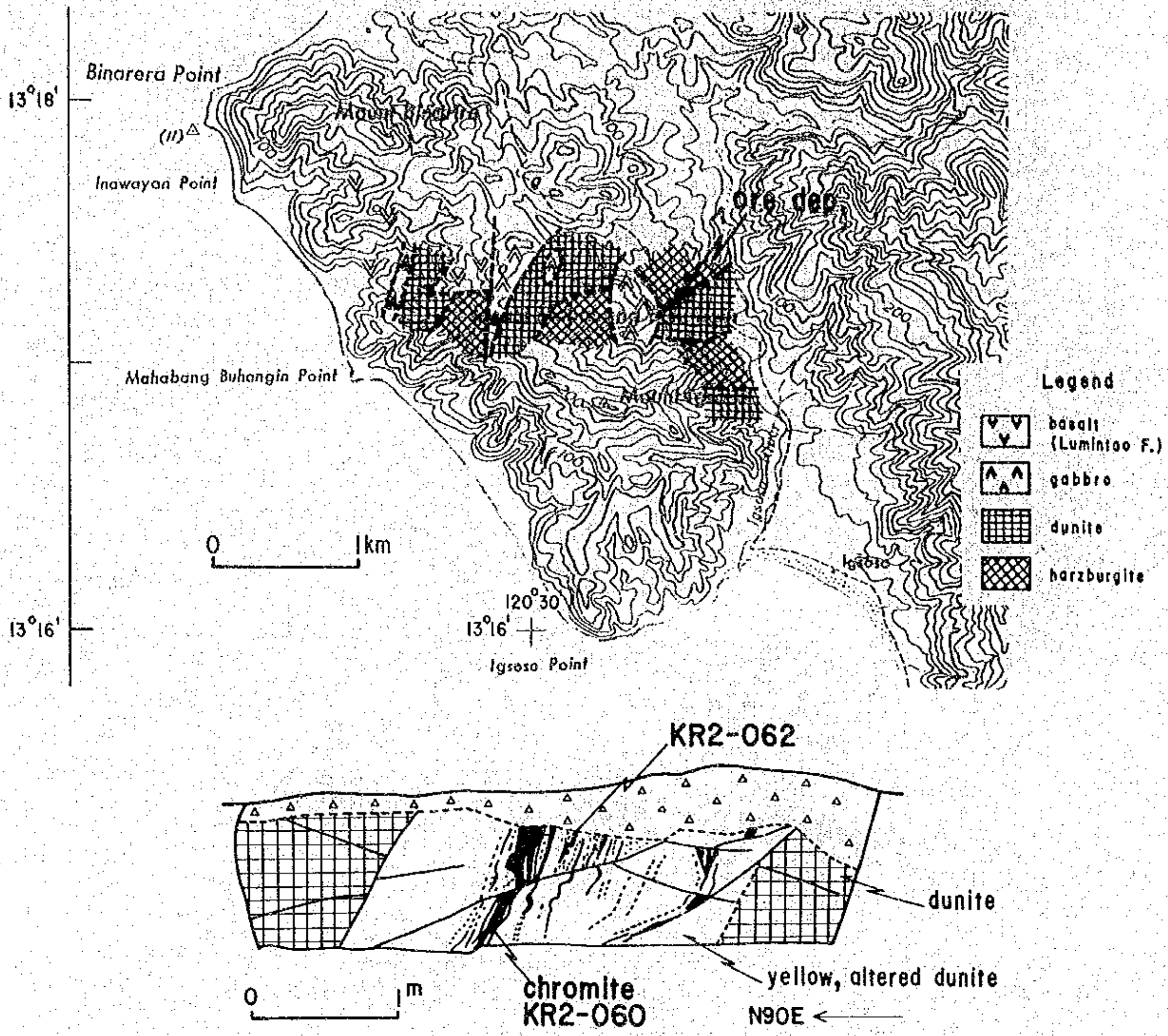

Fig. I-14 Igsoso Chromite Deposit

The outcrop is found only at the above-mentioned place, but 22 trenches are found in the surrounding area of gabbro, and about 10 tons of stockpile consisting of massive, spotted, banded and disseminated ores remain there. As a massive ore of the maximum diameter of 0.65 m is found, the ore body might have partly swelled.

Under the microsope, chromite in the banded ore of the outcrop, commonly has an anhedral, granular form of 0.03 to 1.0 mm long. Euhedral crystals are also observed in a small amount. Inclusions (0.01 to 0.03 mm in size) of silicate minerals (olivine) are often zonally arranged in the crystals. Prismatic to acicular crystals (0.01 to 0.1 mm wide and 0.1 to 1 mm long) of magnetite are observed in a very small amount and are partly hematitized. They are strongly brecciated by shearing.

Analytical values:

Sample No.	Thick-ness m	Cr_2O_3 %	Fe %	SiO_2 %	Al_2O_3 %	MgO %	Ni %	Co ppm
KR2–60 (banded ore)	0.15	34.14	8.57	13.14	5.88	14.14	0.08	26
KR2–62 (banded ore)	0.05	38.85	10.14	13.92	4.29	10.89	0.16	21

Massive ores of the stockpile consist of an aggregate of anhedral chromite, 0.04 to 2.0 mm in size, showing a cataclastic texture. Chromite crystals have been broken to pieces, smaller than 0.2 mm in size, by shearing asshown by numerous wavy structures. Large euheral crystals which are contained in a little amount seem to be rotated by shearing and the peripheral parts are brecciated. Partly hematitized magnetite (smaller than 0.05 mm) and silicate minerals (smaller than 0.1 mm) are included zonally in the crystals.

Analytical values:

Sample No.	Cr_2O_3 %	Fe %	SiO_2 %	Al_2O_3 %	MgO %	Ni %	Co ppm
KR2–065 (massive ore) stockpile	42.00	11.29	3.66	9.66	5.99	0.07	28

(D) San Vicente Chromite Deposit (No. 12)

The ore deposit is situated on the top of the small hill and can be reached by five-minutes drive and 20 minutes hike from the highway.

The Ultramafic complex found in the area is small in size (1.5 km x 1.0 km), consisting mainly of harzburgite and it is intruded by augite-hypersthene gabbro and fine-grained diorite (trondhjemite).

The chromite deposit is composed of massive ore bodies of pod shape in harzburgite. The bodies are clearly bounded by small fault or shear zone. (Fig. I–15)

The maximum thickness of 0.40 m is measured in the outcrop, but it might be a width of more than 2 m by the estimation from the size of the boulders. Besides this outcrop, the trenches were excavated at 4 places on the hill top and 5 on the slope. Each of them is about 1 m deep and 10 m long, they seem to be too shallow to reach the bed rock. Under the microscope, the ore of the outcrop consists of euhedral crystals of chromite, 1 – 2 mm in size, and a very small amount of slightly hematitized acicular magnetite (0.01 mm in width), in which shear planes are intersecting each other at about 30°.

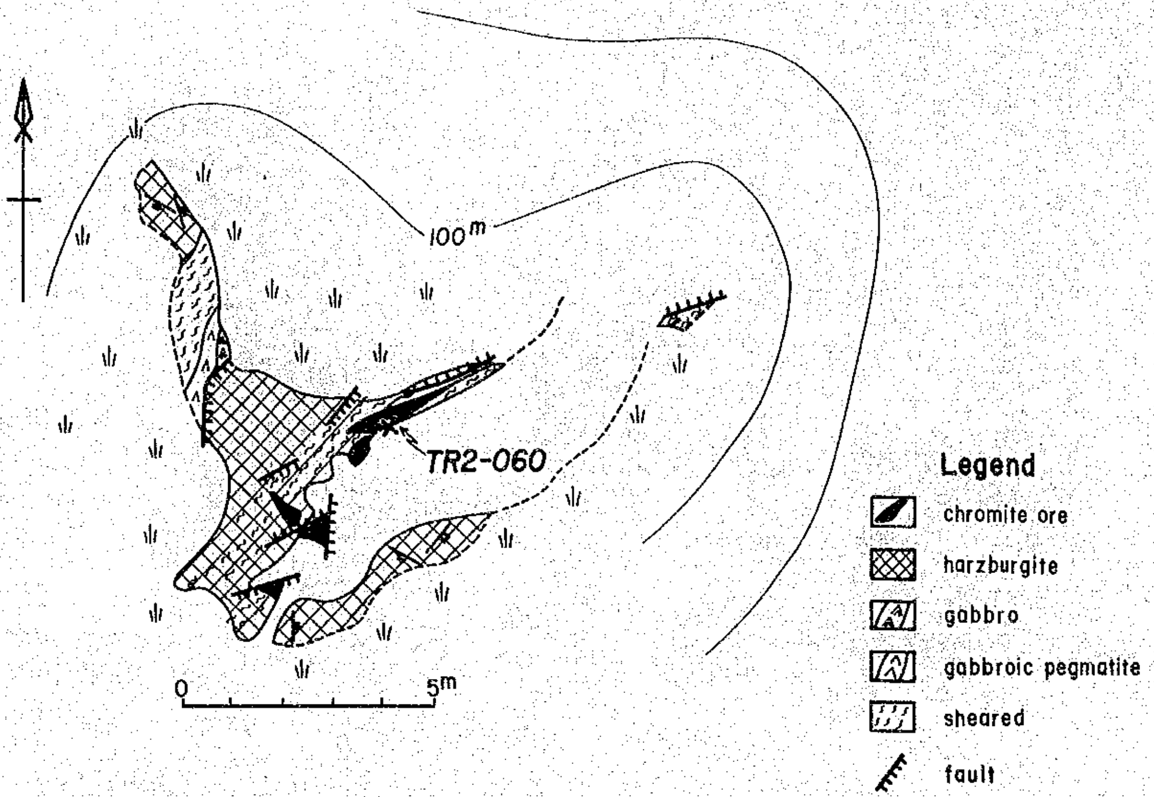

Fig. I-15 San Vicente Chromite Deposit

Analytical values:

Sample No.		Cr_2O_3 %	Fe %	SiO_2 %	Al_2O_3 %	MgO %	Ni %	Co ppm
TR2–060 (outcrop)	massive ore	29.11	10.14	2.38	19.99	8.59	0.08	70
KR2–072 (Boulder in trench)	disseminated ore	5.23	10.29	34.14	1.38	31.45	0.36	164

At present, 3 – 4 tons of ore are stockpiled on the hill top and ore floats of 7 – 8 tons are scattered on the slope. It is said that about 20 tons of ore were shipped several years ago.

The whole neighboring area is the grass land with few rock exposure. However, it is considered that the scale of ore deposit is small from the distribution of boulders of ore and the scale of ultramafic body.

(E) Liwliw Chromite Deposit (No. 57)

The deposit is situated 10 km east-southeast of Mamburao and can be reached by 20 minutes drive and 5 minutes hike along the Mimping River from Mamburao.

The ultramafic body in the area is on a small scale with 8 km long in the E–W direction and 1 – 3 km wide and intruds into the Lumintao and Mansalay formations.

They are mainly composed of peridotite (harzburgite and lehrzolite) > dunite > hornblendite, which are associated with gabbro on both sides, and all of these rocks are strongly altered and weathered.

In the area of the ore deposit, wavy beds of lehrzolite and dunite are distributed in harzburgite (?) in the lenticular form, trending east to west as a whole. The chromite deposit is observed only in harzburgite, arranging almost in parallel with the bedded structure.

Four veins are found on the old mining site. Three pits were excavated. The veins consist of massive to disseminated chromite, 0.03 to 0.15 m in width, showing an irregular form dislocated and distorted by small faults or shear planes. The adjacent part of the veins is notably serpentinized, and the narrow zones of 0.10 to 0.30 cm wide have been altered to yellow in color along the shear plane, small fault and ore vein, which seem to be an important guide for exploration likewise in the Igsoso deposit. (Fig. I–16).

The ore consists of anhedral, granular chromite, 0.01 to 0.1 mm in size, showing a cataclastic texture with abundant irregular cracks.

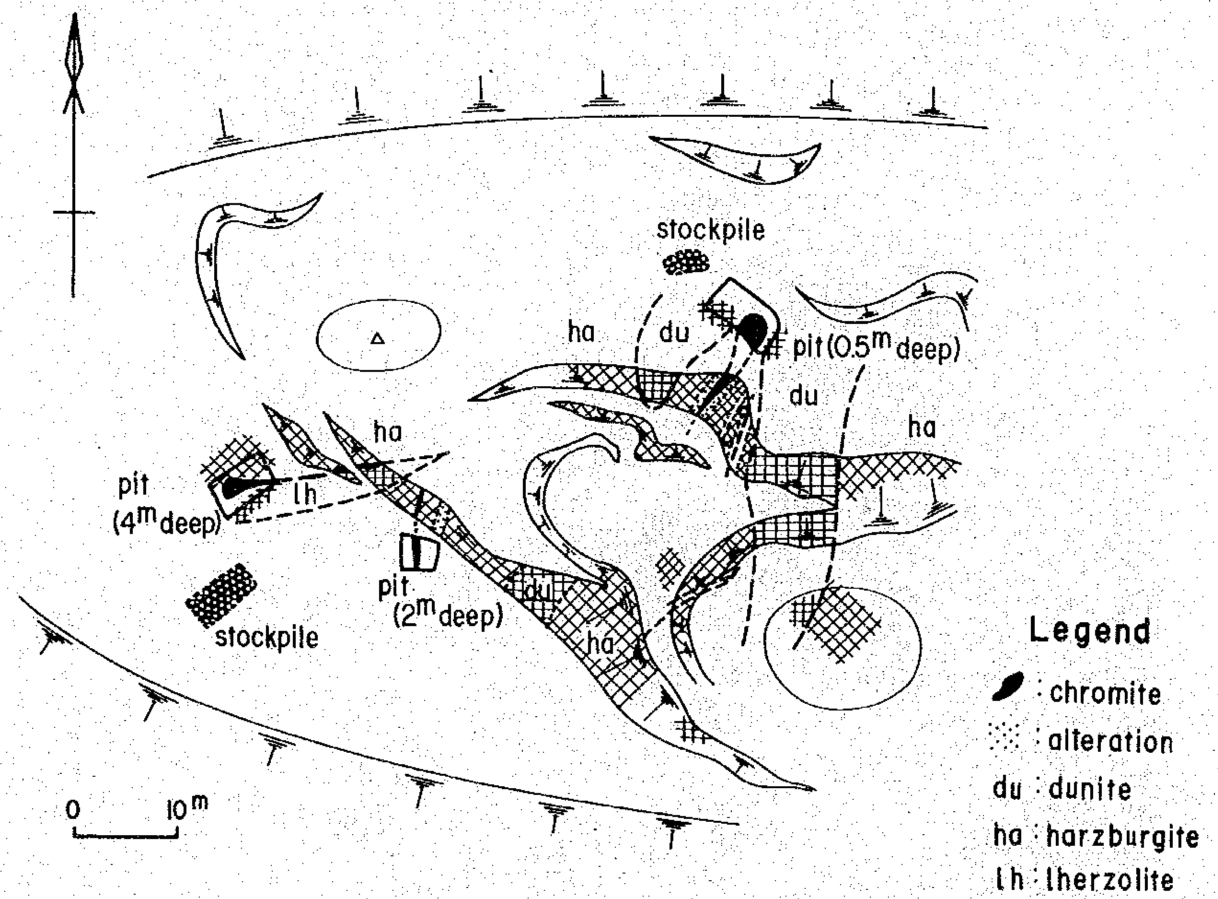

Fig. I-16 Liwliw Chromite Deposit

About 20 tons of ore are stockpiled near the pits with the ore blocks of 0.40 m in maximum diameter.

Analytical values of the stockpile:

Sample No.	Cr_2O_3 %	Fe %	SiO_2 %	Al_2O_3 %	MgO %	Ni %	Co ppm
KR2–055a (spotted ore)	40.31	4.00	5.72	10.68	6.78	0.04	17
KR2–055b (massive ore)	36.50	7.86	7.78	9.39	9.37	0.03	13

(F) Paragpagan Nickel Deposit (No. 16)

The deposit is a nickeliferous laterite deposit distributed on the top of the mountain at Paragpagan, 12 km east of Sta. Cruz. The area is in the center of the Pintin ultramafic body, consisting mainly of harzburgite.

The deposit was investigated in the past by means of soil sampling by BMG, rock and soil sampling by Vulcan Mining and Industry Corporation and pitting by Almeda Mining (Fig. I–17).

From the observation on the surface and in the pits, laterite bed seems to be 2.0 to 2.5 m thick in average. Under the bed, serpentinized harzburgite is broken into blocks and laterite sand fills the interstices between them. Average values of Ni are 0.82 % on laterite and 0.79 % on laterite sand, both of which are not so much different. The similar values were obtained from the samples taken in this phase.

Analytical values:

Sample No.		Cr_2O_3 %	Fe %	SiO_2 %	Al_2O_3 %	MgO %	Ni %	Co ppm
SR2–042	laterite sand	1.82	22.43	9.46	3.38	10.79	0.69	422
SR2–044	laterite	2.66	45.43	2.28	2.44	0.73	0.92	1,418

The laterite reserve comes to about 4.3 MT, when the area is 120 ha with an average depth of 3 m.

(G) Pintin Chromium Deposit (No. 58)

The deposit is situated on the ridge on the northwester side of the Amnay river, about 20 km northeast of Sablayan. It takes about 1 hour to get there on foot from the highway. In this area a ultramafic body extends in the direction of NW–SE with a width of 2.5 km. Augite-hornblende gabbro, augite-hypersthene gabbro, harzburgite and orthpyroxenite are zonally arranged successively from the southwest. All of them are suffered by strong alteration and weathering.

Although the chromite deposit is emplaced in harzburgite, thin lenses of dunite may occur near the deposit.

Many floats are found on the slope and the ridge, where trenching was carried out at three

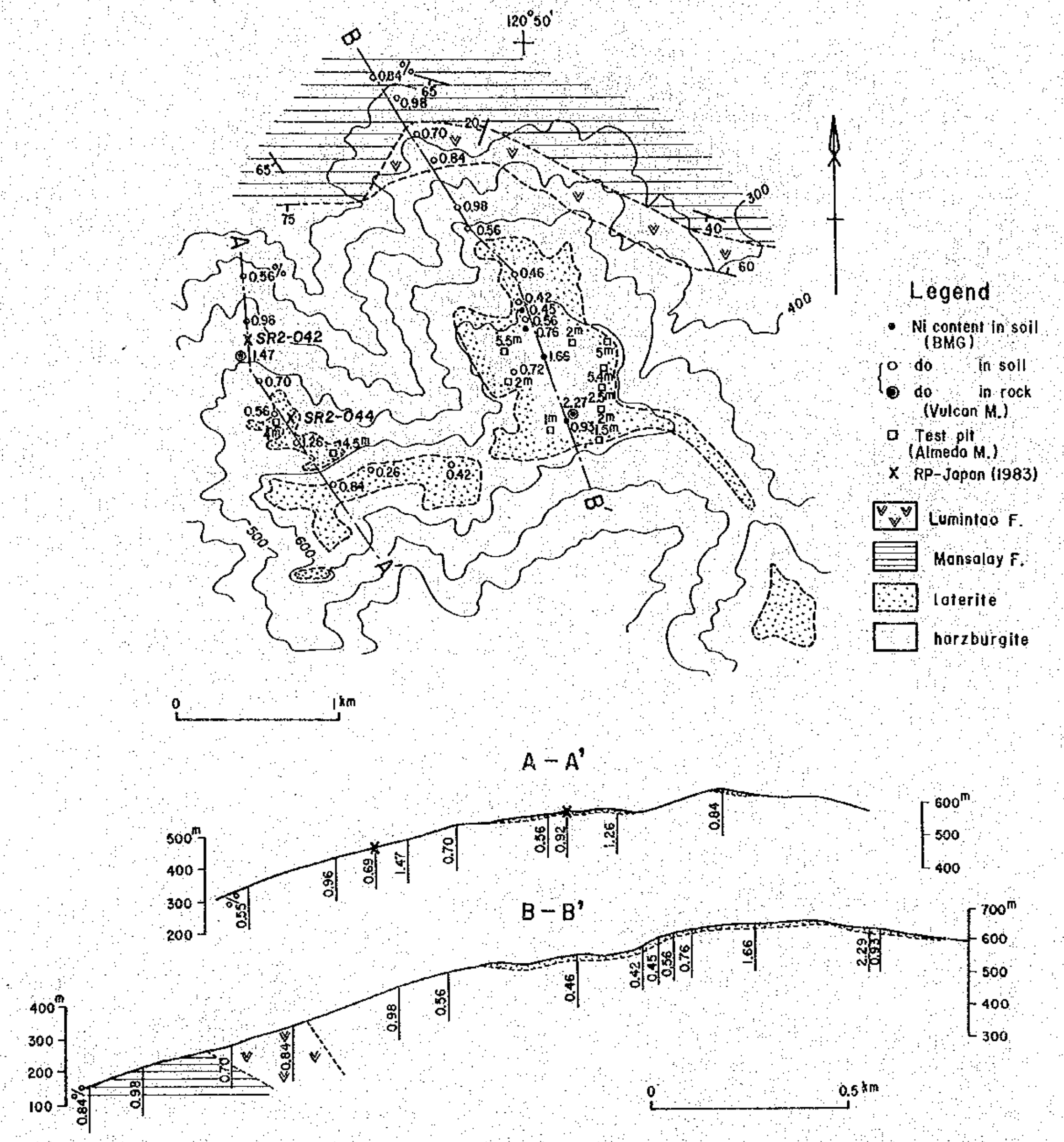

Fig. I-17 Paragpagan Nickeliferous Laterite Deposit

places. As the distribution of the floats is limited within 100 meters along the slope, the deposits may be on a small scale. From the location and mode of occurrence of the floats, two (?) ore bodies can be emplaced about 500 m apart, though their shapes are not clear. About 5 tons of massive to disseminated ore are stockpiled on the site, among which the maximum ore measures 0.40 m in diameter.

The ore mineral mostly consists of euhedral chromite, 0.2 to 1.0 mm in size, with a little irregular cracks.

Analytical values of float ores are as follows.

Sample No.	Cr_2O_3 %	Fe %	SiO_2 %	Al_2O_3 %	MgO %	Ni %	Co ppm
KR2–050a	50.03	14.57	4.00	5.35	4.63	0.09	19
KR2–050b	53.55	15.29	2.24	4.69	2.42	0.07	16

(H) Other Chromite Deposits

Chromite deposits were found at two places in the ultramafic body in the vicinity of Paluan, both of which are small in scale.

(H)–1 Marri Deposit (No. 54)

The deposit is exposed on the small ridge on the northern side of the Paluan River, 6 km east-northeast of Paluan, consisting of massive to disseminated ore of 0.70 m wide. Because of poor exposure, serpentinite body of the country rockcan hardly be checked, which appears to be small in size.

Ore mineral is only chromite, which is not subject to shearing, though parallel cracks are found.

Analytical values:

Sample No.	Cr_2O_3 %	Fe %	SiO_2 %	Al_2O_3 %	MgO %	Ni %	Co ppm
YR2–037a (massive ore)	40.31	10.00	8.44	6.65	6.45	0.06	20

(H)–2 Mariil Deposit (No. 55)

The deposit was described as the Paluan chromite deposit in the Phase I report. It was made clear by the Phase II survey that the ultramafic body has an area of 2 km x 1 km consisting of harzburgite $\gg$ dunite and is intruded by gabbro and fine-grained diorite (tronhjemite) on a small scale, and that the rock type and rock series are almost same as those of Liwliw and Igsoso.

Besides the ore stockpile reported least year, some pebbles were newly found in the small creek, 1 km north from the stock pile, and on the mountain slope, but the shape of ore body is not clear.

The ore is massive to disseminated and high-grade.

The analytical values of typical ores are as follows.

Sample No.	Cr_2O_3 %	Fe %	SiO_2 %	Al_2O_3 %	MgO %	Ni %	Co ppm
KR2–069a (stockpile)	50.50	10.14	4.48	6.69	4.38	0.02	4
KR2–069b (do)	45.82	10.86	5.74	5.57	5.07	0.02	5
KR2–070 (boulder)	48.93	10.00	1.22	6.75	2.88	0.02	8

2–2–3 Iron Ore Deposits

Many iron ore deposits are scattered in the limestone area near the ridge in the northern part of the central mountain range. The deposits are of a contact metasomatic type, consisting mainly of magnetite and hematite with skarn minerals. Six iron ore deposits were checked in the upper stream of the Mamburao River during this survey (Fig. I–18). In order to get this deposit area no other course can be found than either taking a steep mountein trail from Abra de Ilog or going up the Mamburao River with great boulders. Walking along either way is so difficult that it takes at least two days to get there.

The outline of the ore deposits is as follows.

(A) Nagsabongan deposits (No. 29)

Two outcrops are found on the northern slope of the Nagsabongan creek, the eastern tributary of the Mamburao River. No.1 outcrop (690 m above sea level) is 50 m wide and extends more than 50 m laterally. No.2 outcrop (740 m above sea level) is located 70 m apart from the No.1 outcrop, having a width of more than 20 m. Although the relation between the both outcrops and the country rock are not clear, they appear to be the same deposit and are considered to be emplaced in limestone of the Sablayan group in the bedded form (striking NE–SE and dipping 40° S). (Fig. I–19).

The ore minerals mostly consist of magnetite. Microscopically a small amount of hematite which replaced along the cracks in magnetite in the acicular or dendritic form and a very small amount of fine-grained (0.02 mm in size) pyrite and chalcopyrite are also observed. The iron ore is porous in places, suggesting leaching of the skarn minerals.

The ore is a high grade ore with little impurity.

Sample No.	Fe %	SiO_2 %	Al_2O_3 %	S %	P %	TiO %	As %
FR2–036(No.1 outcrop)	6.136	0.98	0.30	0.07	0.023	0.011	0.011
FR2–037(No.2 outcrop)	60.82	0.80	0.30	0.03	0.019	0.014	0.017

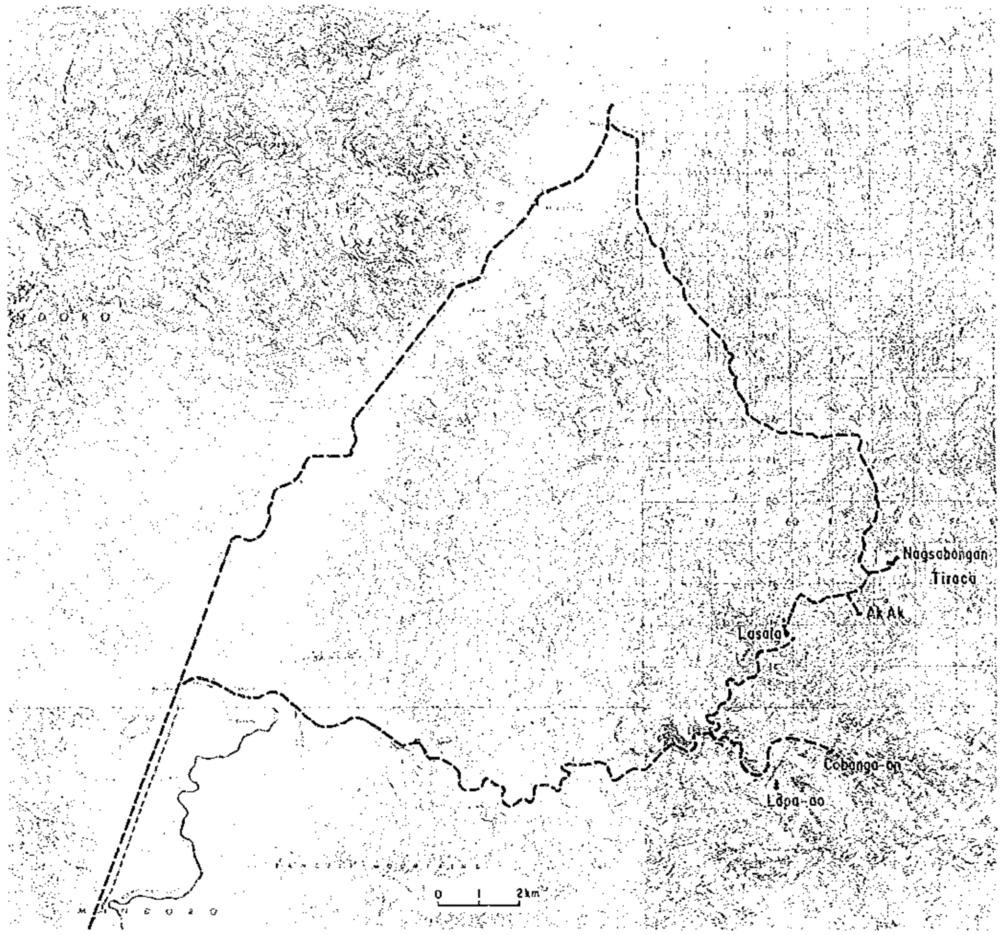

Fig. I-18 Location Map of Iron Deposits, Mamburao River Area

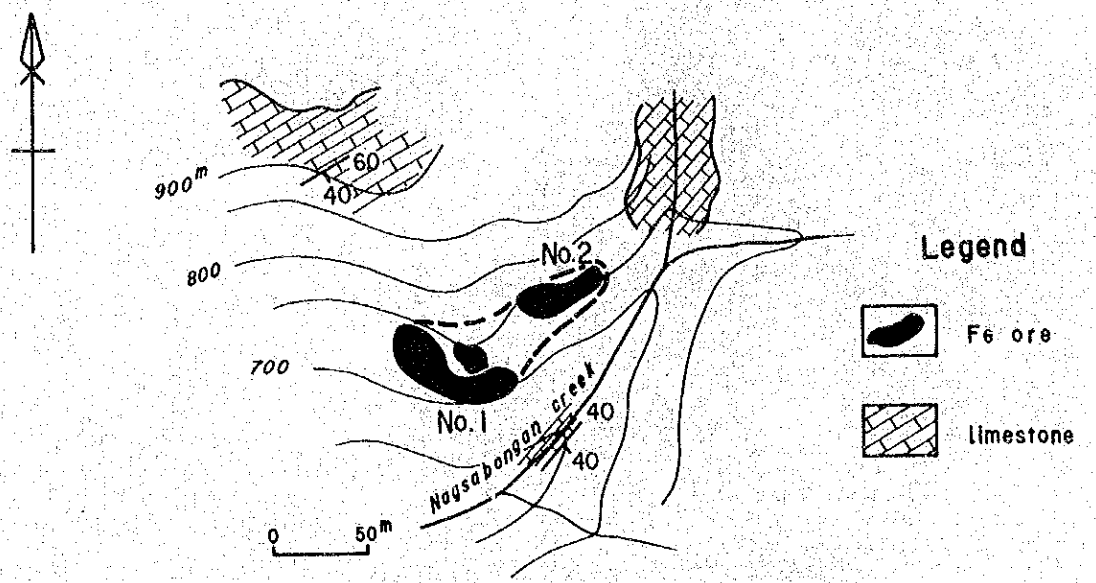

Fig. I-19 Nagsabongan Iron Deposit

The Elizalde Co. carried out exploration on the deposit from 1962 to 1965 by magnetic survey, trenching, drilling and tunneling. It is said that the extension of the deposit is 92 m x 65 m and the thickness of 35 meters at the center. No details, however, are available.

At a rough estimate of the ore reserve based on the result of the Phase II survey the tonnage is about one million tons above No. 1 outcrop level (L = 120 m, W = 50 m, and H = 50 m).

(B) Lasala deposit (No. 30)

The deposit is situated at a place of 400 to 460 m above sea level in the upper stream of the Mamburao River, about 3 km WSW of the Nagsabongan deposit.

Near the ore deposit, limestone of the Salayan group forms a steep cliff at the high place of more than 600 m above sea lvel and a gentle slope consisting mainly of skarn continues to the river bed. Eocene to Oligocene quartz diorite is exposed at the bed of the river in

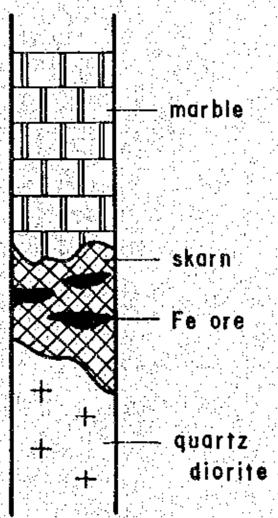

Fig. I-20 Schematic Columnar Section of Lasala Area

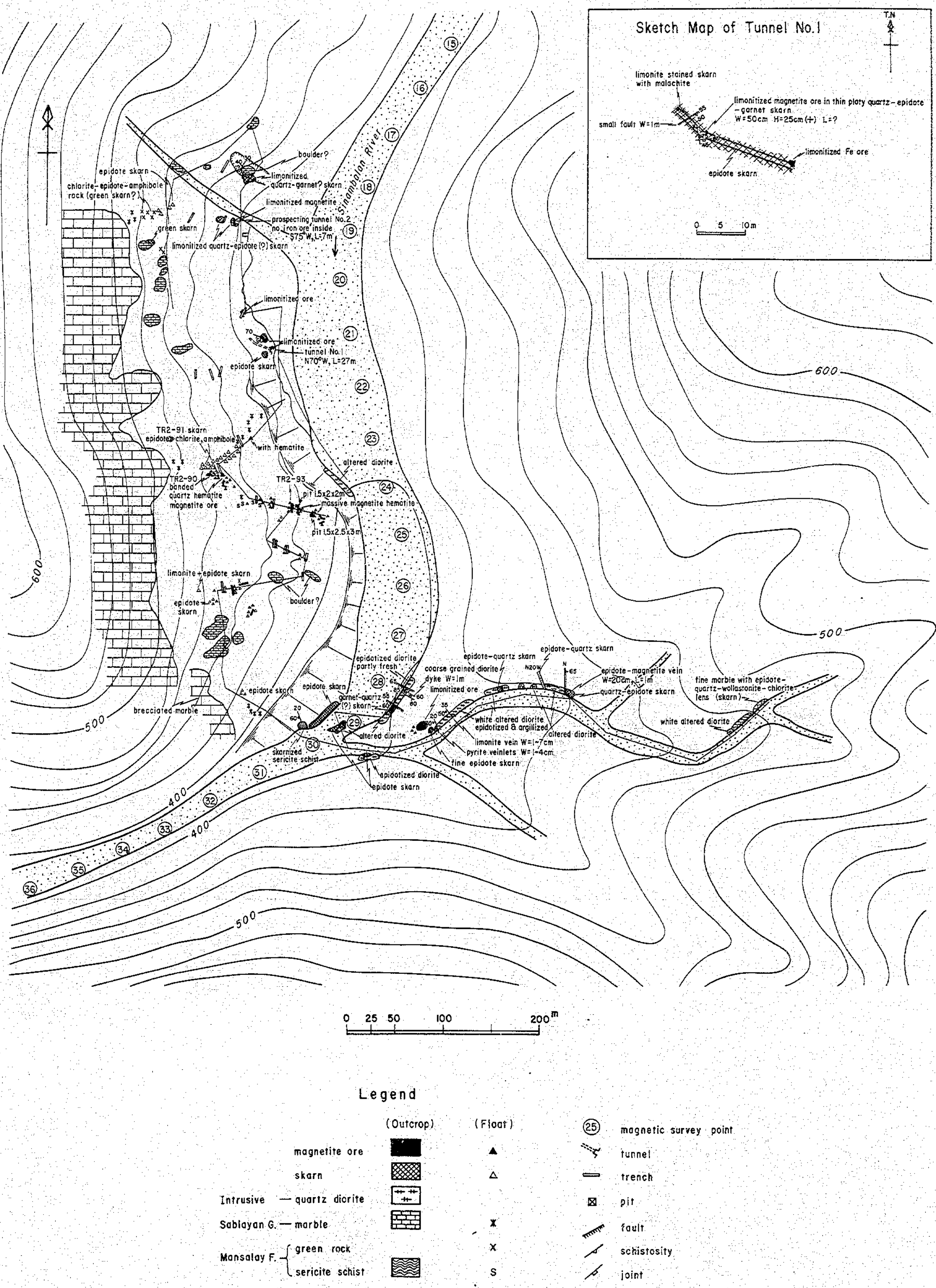

Fig. I-21 Route Map of Lasala Area

the stock-like form. Sericite schist and amphibole schist of the Halcon metamorphics are exposed in a limited area, which is likely to be a xenoblock in quartz diorite.

As shown in Fig. I–20, the massive iron deposit is emplaced in the lenticular or irregular form in limestone which is skarnized by the intrusion of quartz diorite. A reserve of one unit ore body seems to be some tens thousnad tons to some hundreds thousand tons.

Fig. I–21 shows the geology and ore deposits of the Lasala area. The area composed of the skarn containing the ore deposits has an extent of 150 m (E–W) x 600 m (N–S) at the foot of mountain on the western bank of the Mamburao River. The ore deposits and the floats are concentrated within an area of 130 m (E–W) x 100 m (N–S) in the center of the above-mentioned area.

The ore is commonly composed of compact and massive magnetite, associated with a small amount of skarn minerals. Magnetite, hematite and quartz sometimes show a banded structure. Specularite is found in some places in quartz veinlets filling the cracks in the ore.

Under the microscope, magnetite (0.05 mm in average grain size) has been replaced by almost same amount of hematite, showing that hematitization in Lasala is stronger than that in Nagasabongan. Sulphide minerals are hardly observed.

Assay results of the typical ores:

Sample No.		Fe %	SiO_2 %	Al_2O_3 %	S %	P %	TiO_2 %	As %
TR2–093	(massive ore)	49.09	19.88	0.25	0.02	0.055	0.004	0.002
TR2–090	(banded ore)	28.23	53.60	0.36	0.52	0.025	0.024	0.021

As regards the skarn, epidote skarn is most abundant followed by garnet skarn. Diopside, amphibole and wollastonite are also observed, though very small in amount.

The area was once explored by Mayorga Mining Company from 1961 to 1964. In this survey, two tunnels (27 m and 7 m in length), two pits (1.5 m x 2 m x 2 m and 1.5 m x 2 m x 3 m) and 24 trenches (10 m in an average length with less than 0.5 m depth) were confirmed. No trace of drilling, however, could be found. These exploration seems to have dug down the overburden where the ore floats were concentrated rather than to have investgated the lateral or vertical extension of the outcrops.

(C) Lapa-ao deposit (No. 32)

The deposit is found in the upper stream of the Lapa-ao River, the southern tributary of the Mamburao River, 500 to 600 m abovesea level. It is situated about 3.5 km south of the Lasala deposit.

The surrounding area is composed of phyllite, green phyllite, limestone and dolomite of the Mansalay formation, and limestone of the Sablayan group, unconformably overlies the above formation.

The deposits have been formed by replacement of limestone or dolomite of the former formation.

The Sablayan limestone has not been skarnized.

Although any igneous rock closely related to the ore deposit is not exposed in the vicinity, it is considered that quartz diorite is the related rock like the Lasala deposit and would be emplaced in the shallow depth.

Three iron beds intercalated by phyllite are found with thickness of 44 m, 46 m and 28 m from the top along the creek.

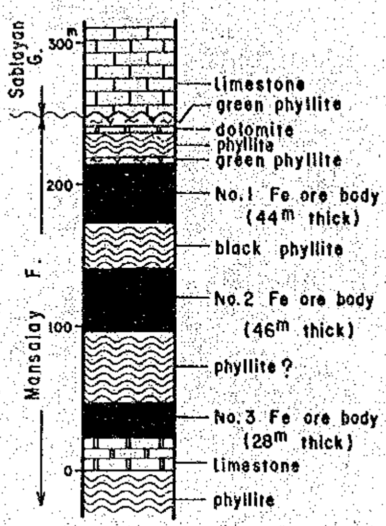

Fig. I-22 Columnar Section of Lapa-ao Area

As shown in Fig. I–22, the extension can not be known in the western part of the creek because they are covered by the Sablayan formation, but they are traceable for 300 – 350 m toward the east trending N50°W with 60°S dip.

Magnetite and skarn minerals commonly compose the ore, and the compact magnetite ore like Lasala is rare in this place.

Magnesian skarn minerals such as talc, sericite and amphibole are found in abundance instead of epidote and garnet.

Under the microscope, the ore consists of an aggregate of magnetite, about 0.3 mm in grain size, and fairly abundant skarn minerals. A very small amount of hematite occur in magnetite in a form of exsolution lamella. Other minerals are hardly observed.

Assay results of the typical iron ore are as follows.

Sample No.		Fe %	SiO_2 %	Al_2O_3 %	S %	P %	TiO_2 %	As %
TR2–096	(No. 1 Ore Body)	52.77	3.30	0.30	0.02	0.017	0.007	0.001
TR2–097	(No. 2 Ore Body)	54.00	6.10	0.40	0.35	0.076	0.011	0.000

From the occurrence of the ore deposits, the extension toward depth can be expected, suggesting reserve of tens million tons class (in case of L=300 m, W=100 m, H=100 m, SG=4.0, reserve is 12MT).

(D) Cobanga-on deposit (No. 63)

The deposit is situated in the upper stream of the Lapa-ao River, 1.5 km east-northeast of the Lapa-ao deposit. The altitude is 470 meters.

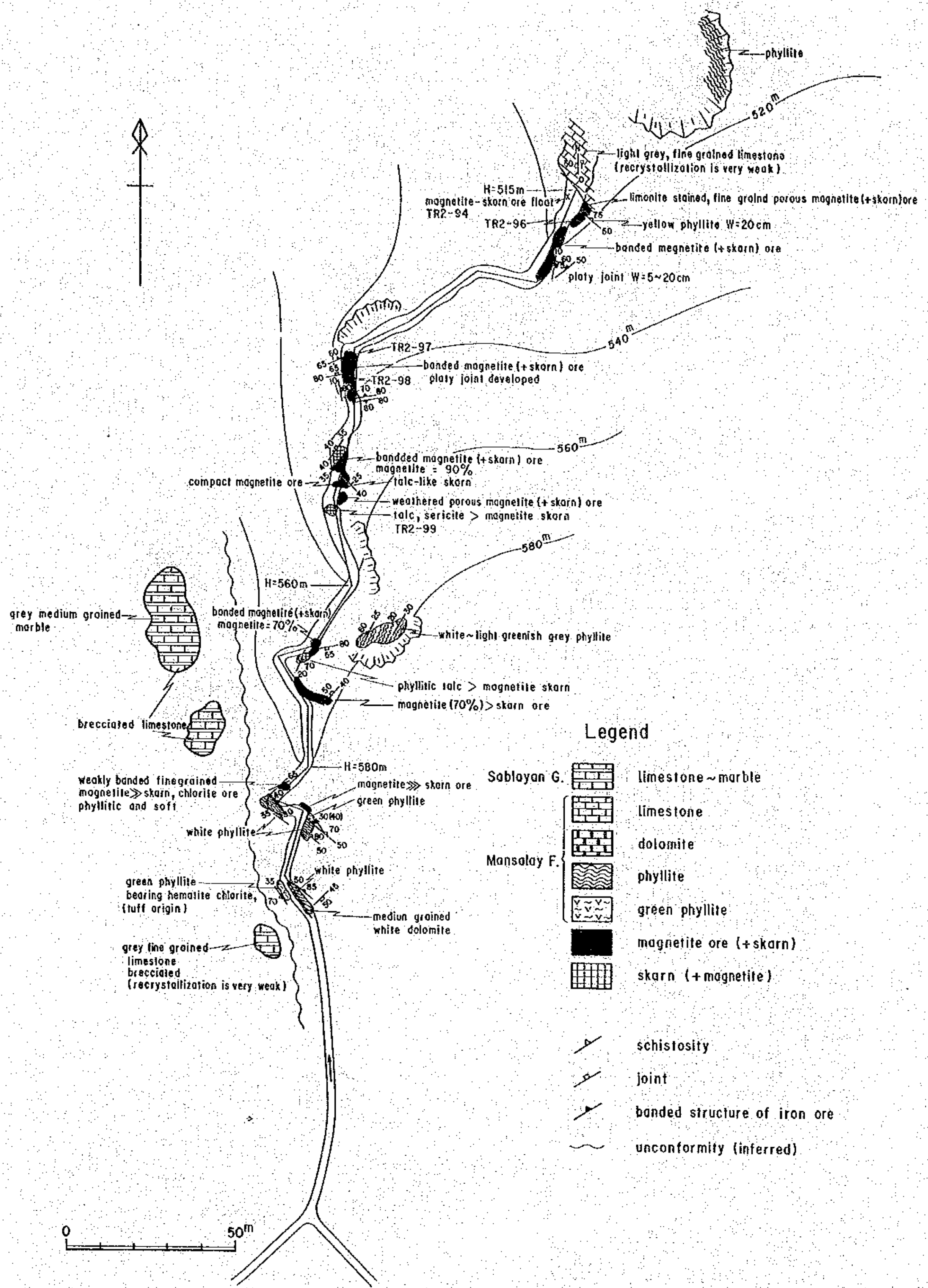

Fig. I-23 Route Map of Lapa-ao Area

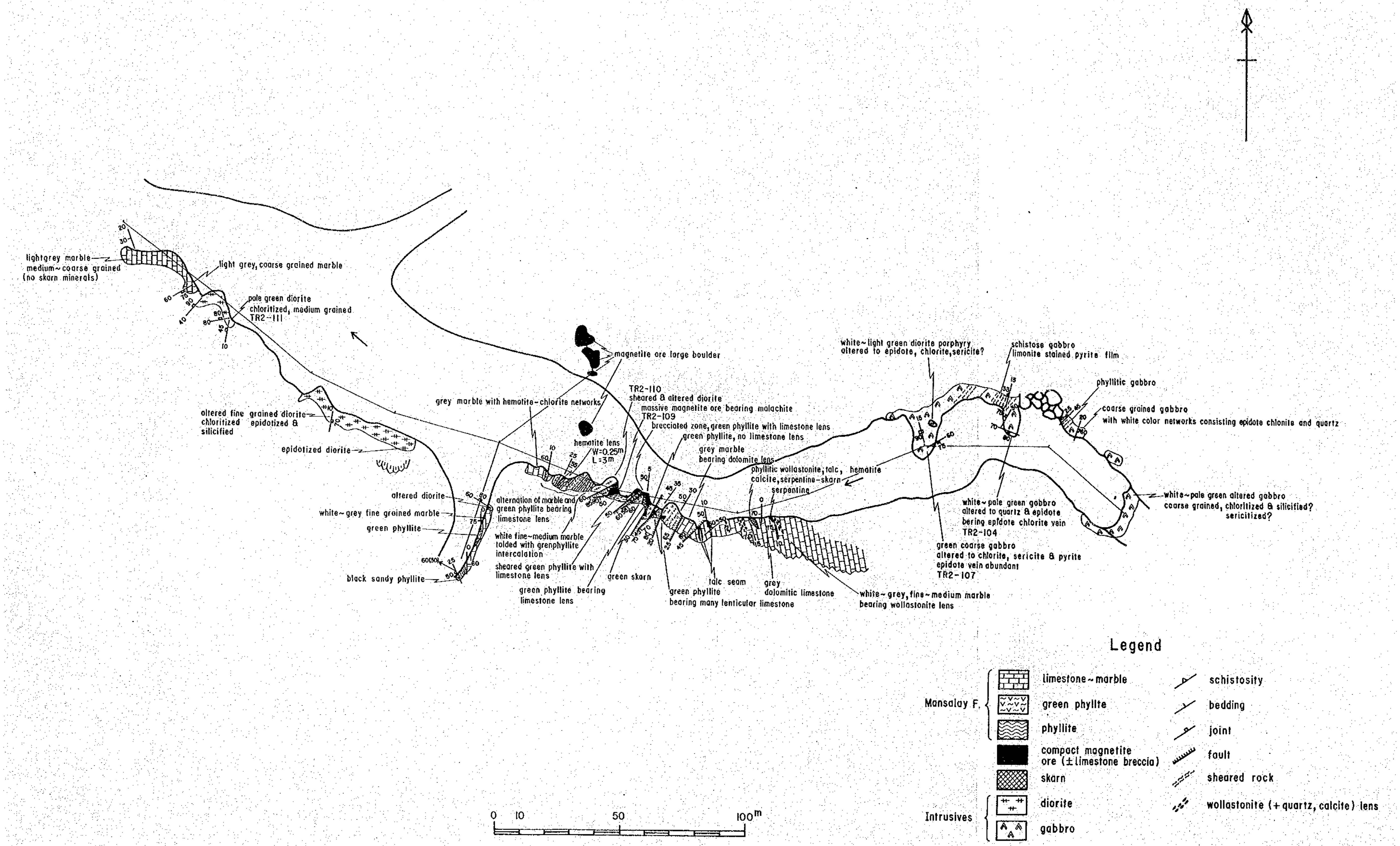

Fig. I-24 Route Map of Cobanga-on Area

The area consists of limestone, green phillite and black phyllite of the Mansalay formation. Gabbro and quartz diorite have intruded into the formation. Gabbro is a white to pale green, coarse-grained rock and hydrothermally altered to secondary minerals such as chlorite, epidote, sericite, pyrite and quartz. The gabbro seems to intrude into the Mansalay formation in a form of sill. Quartz diorite is a white to pale green, fine to mdeium-grained rock and is hydrothermally altered to abundant chlorite, epidote and quartz.

The deposit is the magnetite deposit which partially replaced the limestone beds intercalated in green phyllite.

Although several lenticular ore bodies, 0.2 to 2.5 m wide and 1 to 3 m long can be observed along the creek, partial swelling can be expected because great boulders such as 7 m x 7 m x 2 m in size are found in the creek.

The ore mineral consists of magnetite as in other deposits, which has been replaced by hematite in the dotted or acicular form. The interstices between magnetite grains are often filled with skarn minerals.

Fig. I–24 shows the occurrence of ore deposit, in which skarn zone is generally narrow. Chlorite, epidote and diopside are characteritically observed in the ore-bearing green phyllite beds, while wollastonite, quartz, calcite, talc and tremolite occur in the lower crystalline limestone.

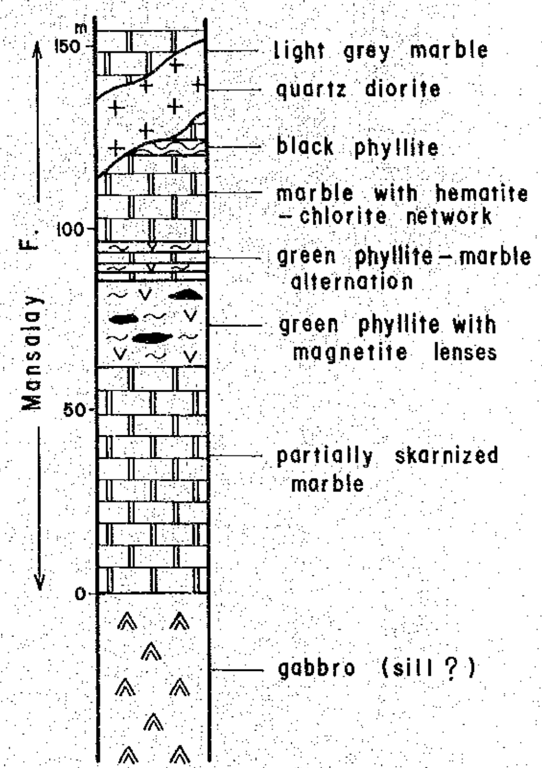

Fig. I–25 Columnar Section of Cobanga-on Area

Assay result of typical iron ore:

Sample No.	Fe %	SiO_2 %	Al_2O_3 %	S %	P %	TiO_2 %	As %
TR2–109	55.36	7.72	1.02	0.02	0.060	0.028	0.000

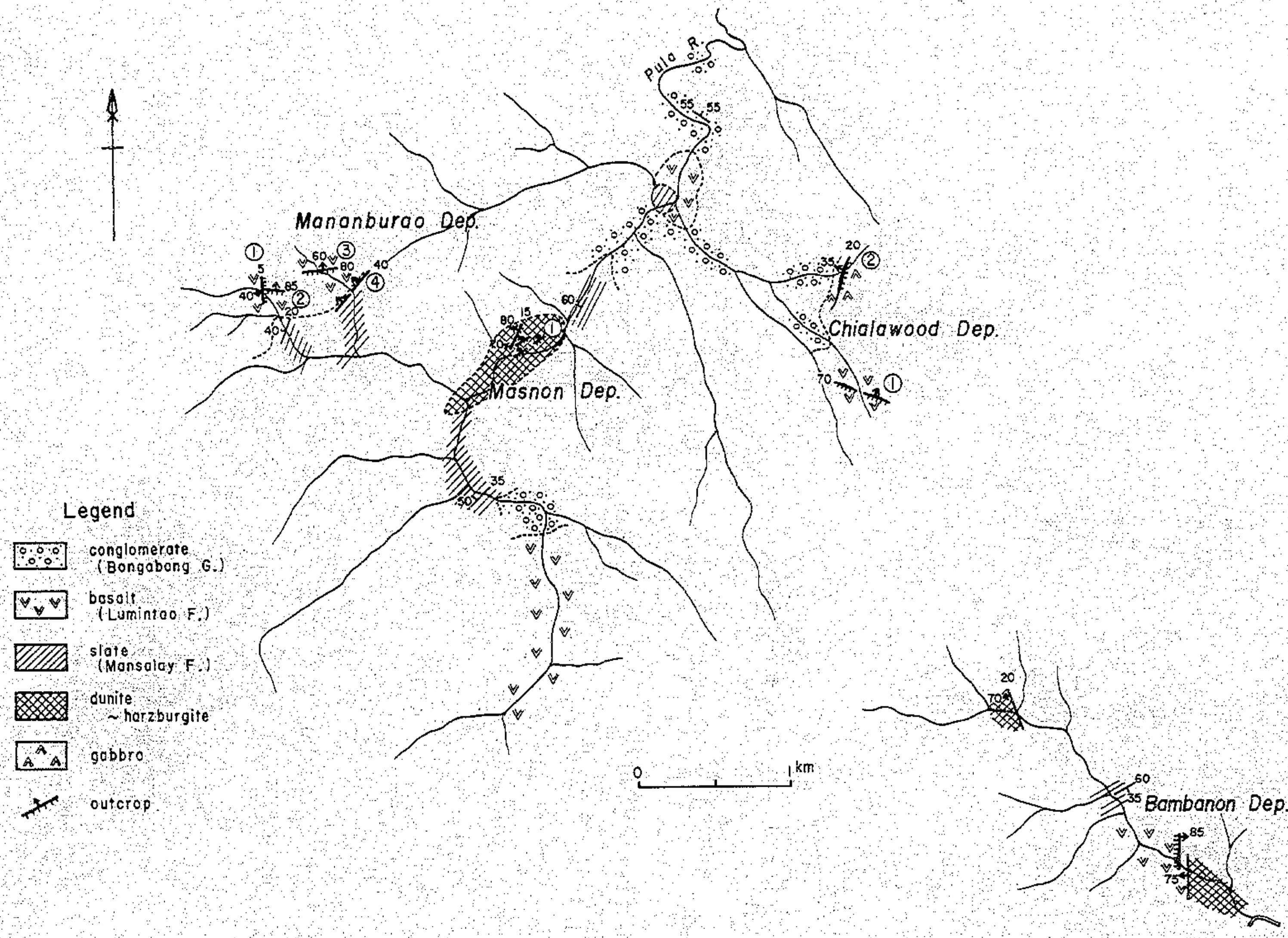

Fig. I-26 Geological Map of Copper Mineralization Area, Pula River